F9180: Diagnostické metody 2

Time-Correlated Single Photon Counting Methods

Tomáš Hoder

Doporučená literatura:

[1] **D.V.O'Connor and D.Phillips** - Time-correlated Single Photon Counting, 1984
[2] **W.Demtroeder** - Atoms, Molecules and Photons, 2006
[3] **W.R.Ware** – Techniques of pulse fluorometry *Time-Resolved Fluorescence Spectroscopy in Biochemistry and Biology (NATO ASI Series A: Life Sciences)* vol 69, ed R.B.Cundall and R.E.Dale (New York: Plenum), 1983
[4] **K.V.Kozlov et al.** 2001 Spatio-temporally resolved spectroscopic diagnostics of the barrier discharge in air at atmospheric pressure, *J.Phys.D:Appl.Phys.* 34 3164
[5] **W.Becker** 2007 Advanced Time-correlated Single Photon Counting Techniques
[6] **W.Becker** 2014 TCSPC Handbook

Overview

- TC-SPC technique/idea
- Time scales, where we can use it, where not
- Light emission, fluorescence, quenching
- Sensitivity, StNR, time resolution, PMT transit
- Use in plasma-physics and synchronization
- Selected examples for gas discharge quantitative spectroscopy

TC-SPC technique

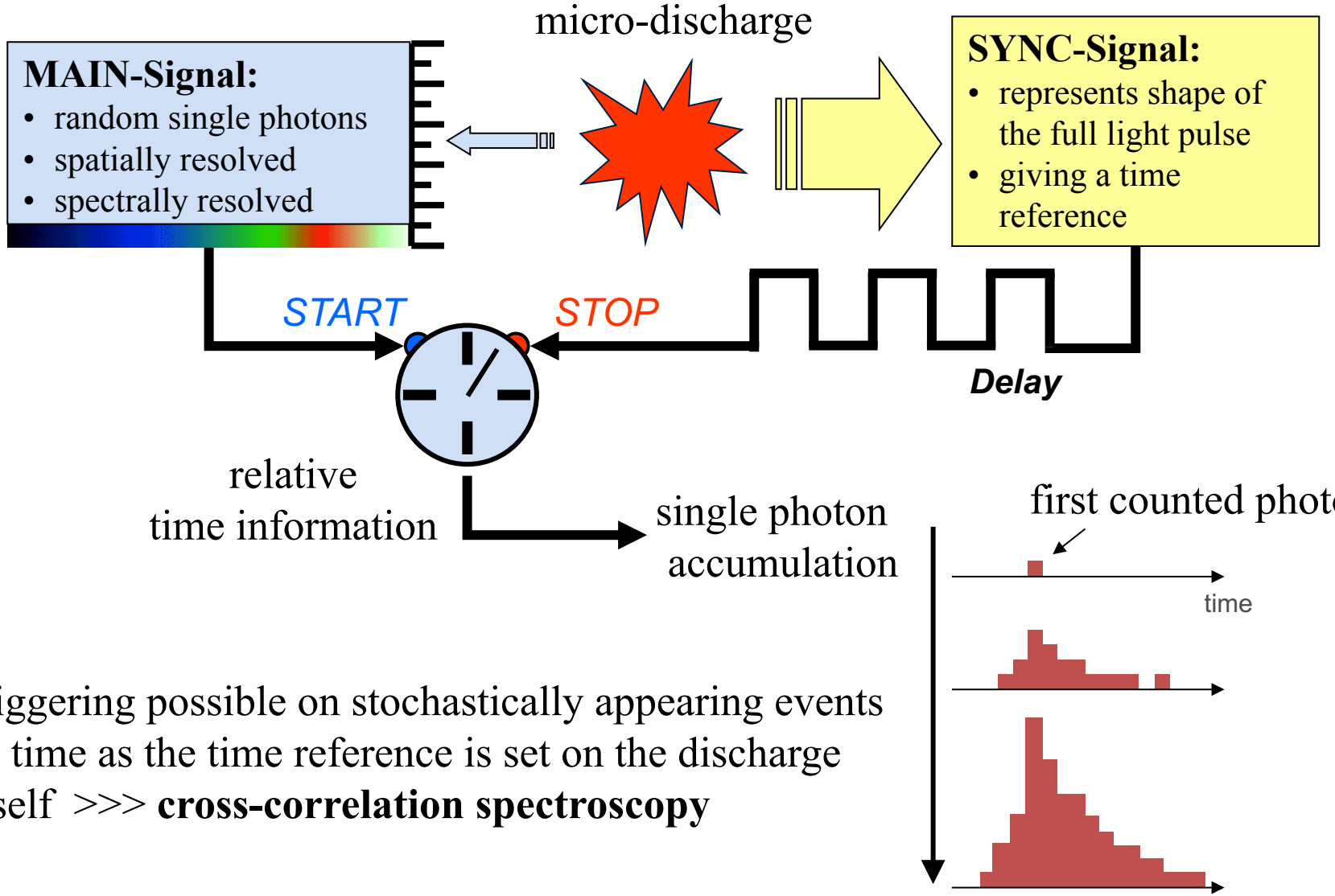

- triggering possible on stochastically appearing events in time as the time reference is set on the discharge itself >>> **cross-correlation spectroscopy**

TC-SPC basics

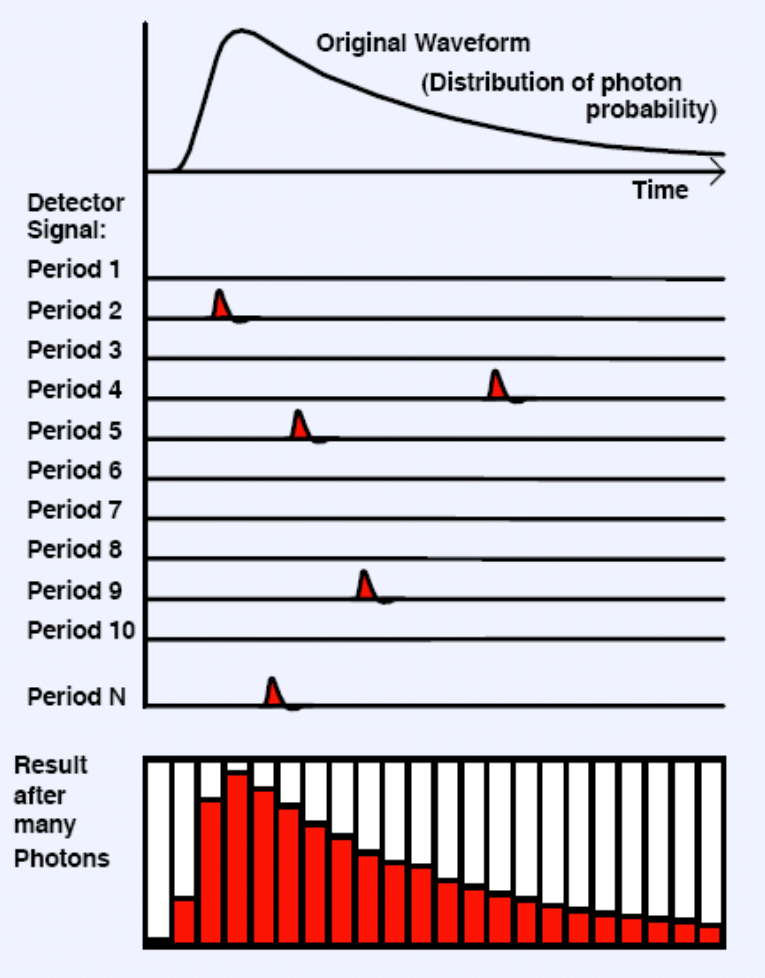

Instead of having problems with slow analogue PMT signal …

TC-SPC obtains light intensity by counting pulses as a digital units in subsequent time channels:

- free of gain noise of PMT
- free of electronic noise of accidental signals to PMT
- high signal-to-noise ratio (to PMT background counting rate)
- higher time-resolution (Transit Time Spread << Single Photoelectron Response/Transit time)

Becker 2006 Advanced TCSPC techniques

Basics

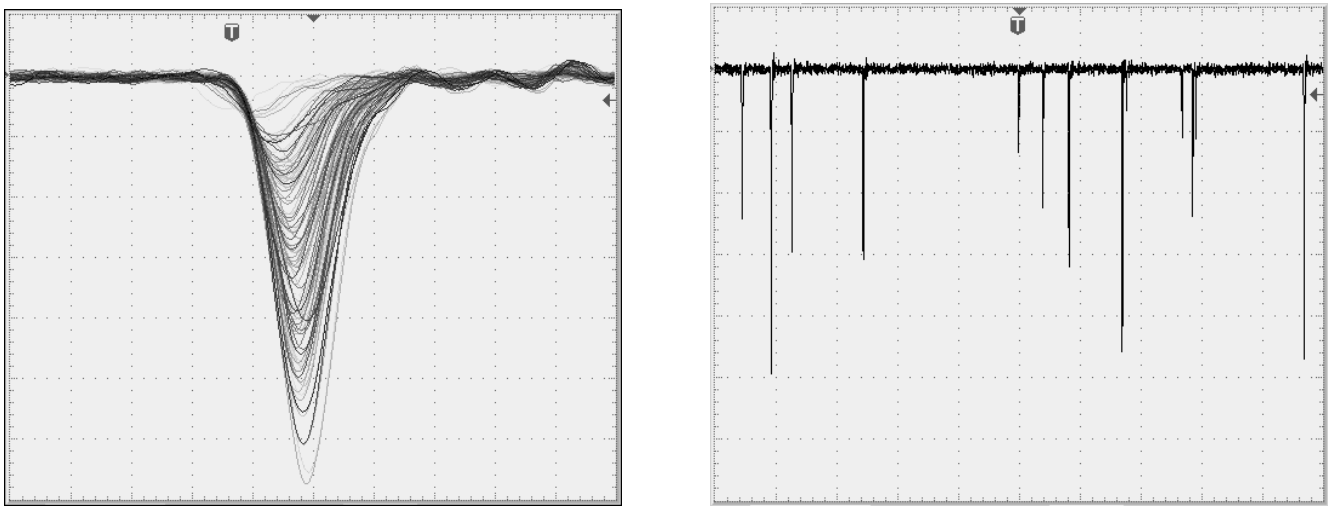

Fig. 102: Single-photon pulses delivered by a R5900 PMT (left, 1 ns / div) and output signal of the PMT at a photon detection rate of 10^7 s^{-1} (right, 100 ns / div). Operating voltage -900V, signal line terminated with 50 Ω.

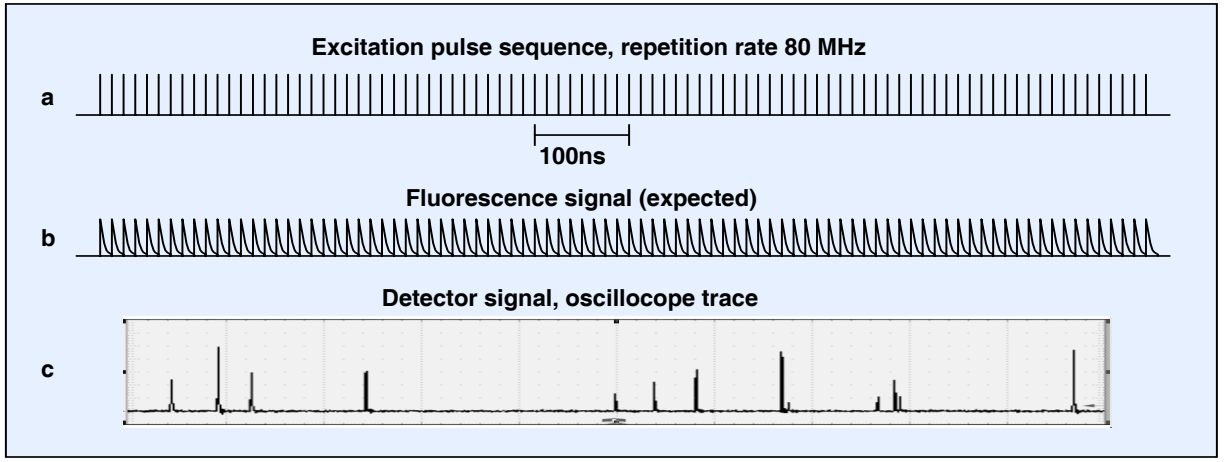

Fig. 103: Detector signal for fluorescence detection at a pulse repetition rate of 80 MHz

TC-SPC solves:

- Problems of triggering/synchro – **recording of irregular emission events**
- Problems of time resolution – **no limitation by transit times or SER of detectors**
- Problems of sensitivity – **statistical principles behind the accumulative recordings**

Convolution -> cross-correlation

1. Express each function in terms of a dummy variable τ.
2. Reflect one of the functions: $g(\tau) \rightarrow g(-\tau)$.
3. Add a time-offset, *t*, which allows $g(t-\tau)$ to slide along the τ-axis.
4. Start *t* at –∞ and slide it all the way to +∞. Wherever the two functions intersect, find the integral of their product. In other words, compute a sliding, weighted-sum of function $f(\tau)$, where the weighting function is $g(-\tau)$.

The resulting waveform (not shown here) is the convolution of functions *f* and *g*.

If *f*(*t*) is a unit impulse, the result of this process is simply *g*(*t*), which is therefore called the impulse response. Formally:

$$\int_{-\infty}^{\infty} \delta(\tau)\, g(t-\tau)\, d\tau = g(t)$$

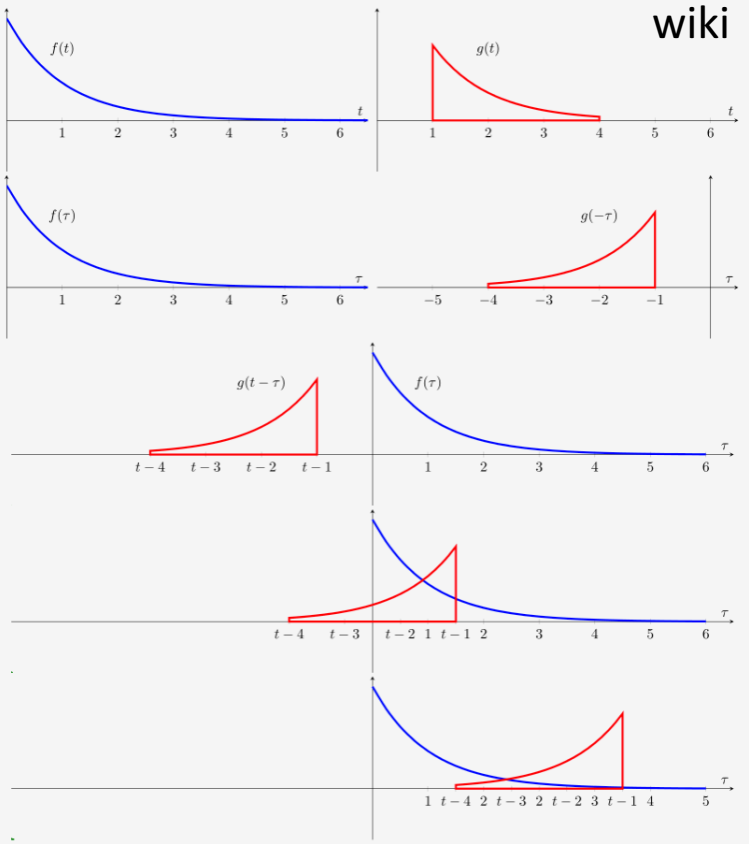

$$(f \star g)(t) \stackrel{\text{def}}{=} \overline{f}(-t) * g(t)$$

$$(f \star g)(\tau) \stackrel{\text{def}}{=} \int_{-\infty}^{\infty} \overline{f}(t) g(\tau + t)\mathrm{d}t$$

$$(f \star g)(\tau) \stackrel{\text{def}}{=} \sum_{t=-\infty}^{\infty} f(t) g(\tau + t)$$

(δ-fce)

Relevant integral transformations:

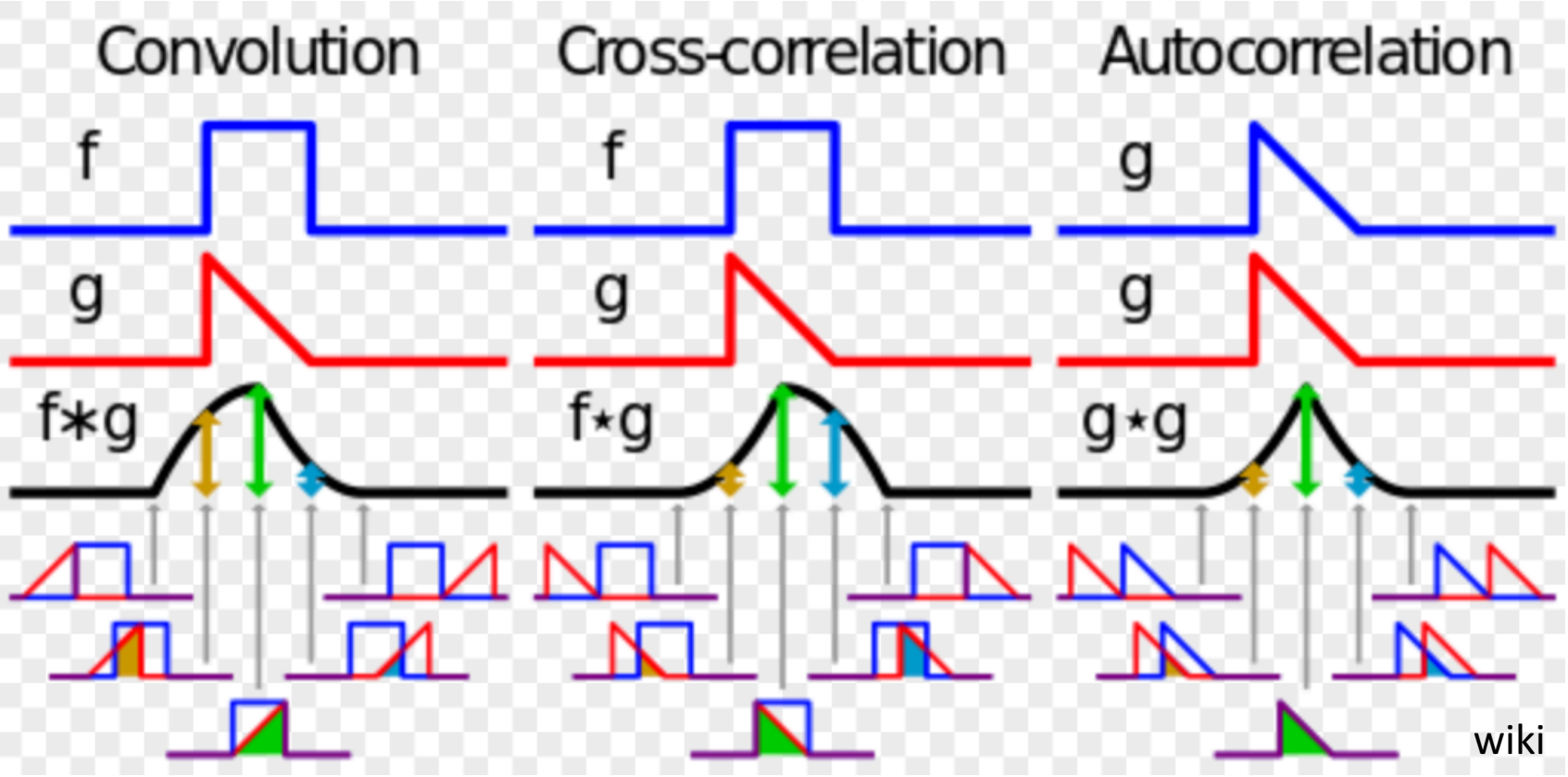

Different time scales and appropriate light detection techniques

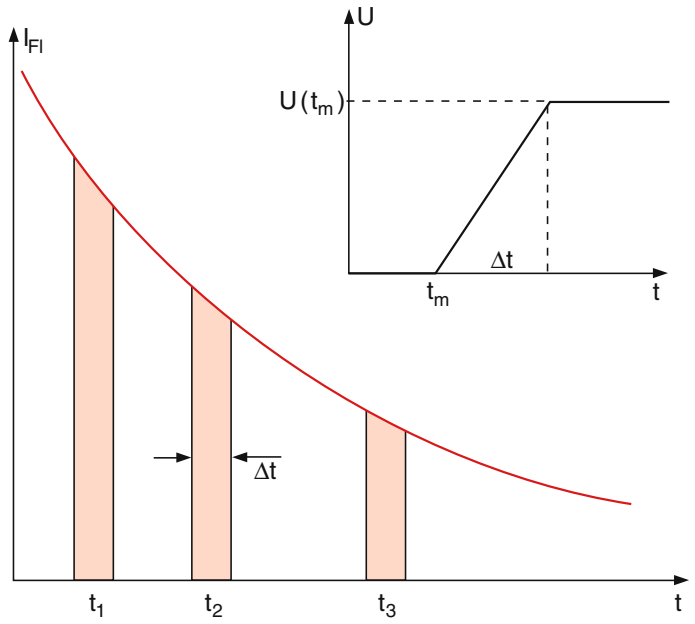

Gated cameras:

- Time resolution from seconds to usually 2ns (new models down to 200 or even 50ps)
- Almost impossible to synchronize to time-irregular emission events (random shot is the time consuming solution)
- Sensitivity of the recording is given by the StNR of given device. Usually the noise increases linearly with number of accumulation cycles. Weak signals are not easy to record.

Different time scales and appropriate light detection techniques

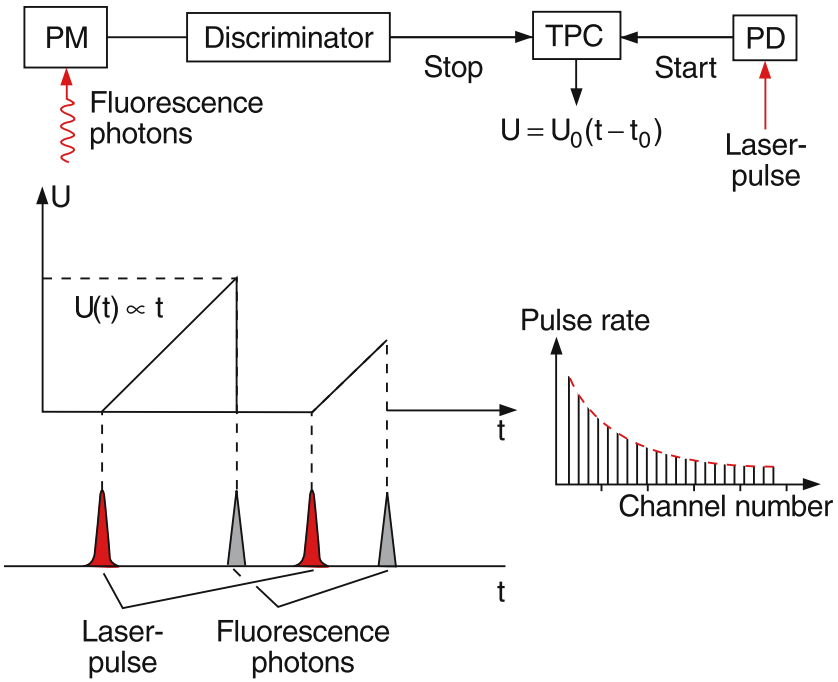

Time-to-amplitude converter
… first time 1961 by Koechlin (Thesis, Uni Paris)

Start-stop TCSPC:

- Time resolution from hundreds of nanoseconds to 10ps
- Possible to synchronize to time-irregular emission events with the same high resolution in time
- Sensitivity of the recording is given by the StNR of given synchronization arrangement. Poisson statistics is the limiting mechanism.
- Limited for high-frequency repetition emission events. Limited by the speed of electronics of the counter dealing with high-frequency input.

Different time scales and appropriate light detection techniques

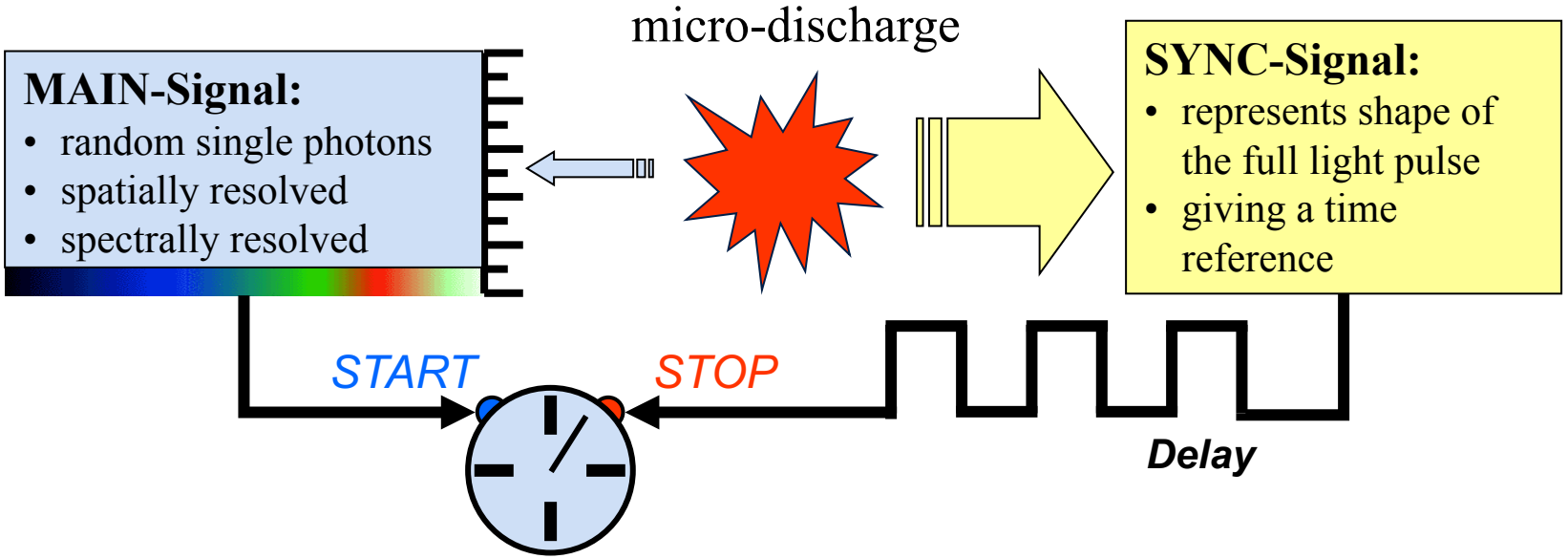

Reversed start-stop TCSPC:

- Time resolution from hundreds of nanoseconds to 10ps
- Possible to synchronize to time-irregular emission events
- Sensitivity of the recording is given by the StNR of given synchronization arrangement. Poisson statistics is the limiting mechanism.
- No limitation for high-frequency repetition emission events. Input processing only for the “main” signal.

Different time scales and appropriate light detection techniques

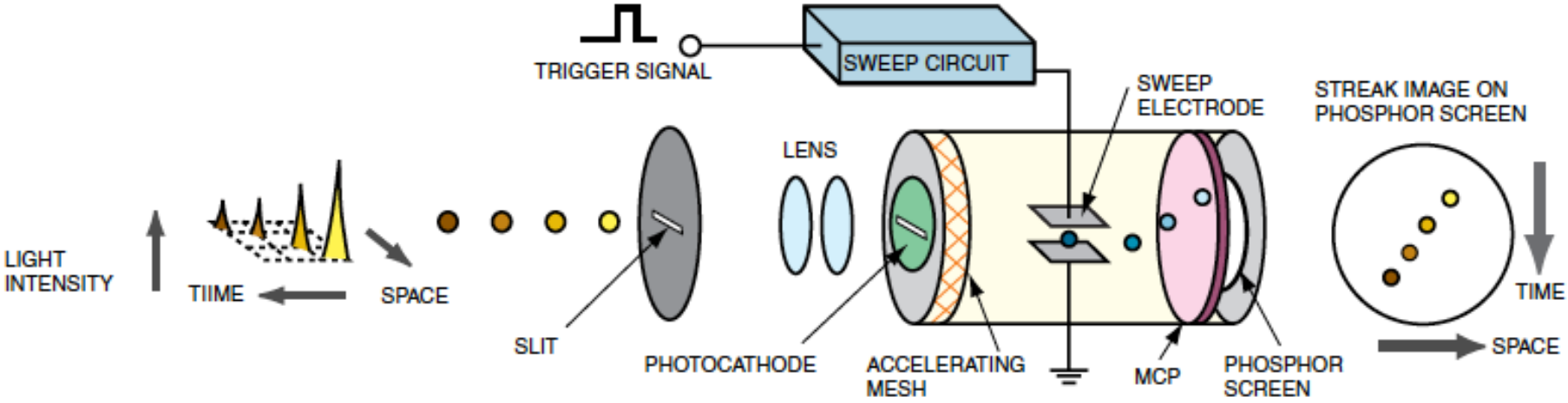

Streak cameras:

- Time resolution down to units of picoseconds (some new models down to hundreds of femtoseconds)
- Sensitivity of the recording comparable to the TC-SPC

Different time scales and appropriate light detection techniques

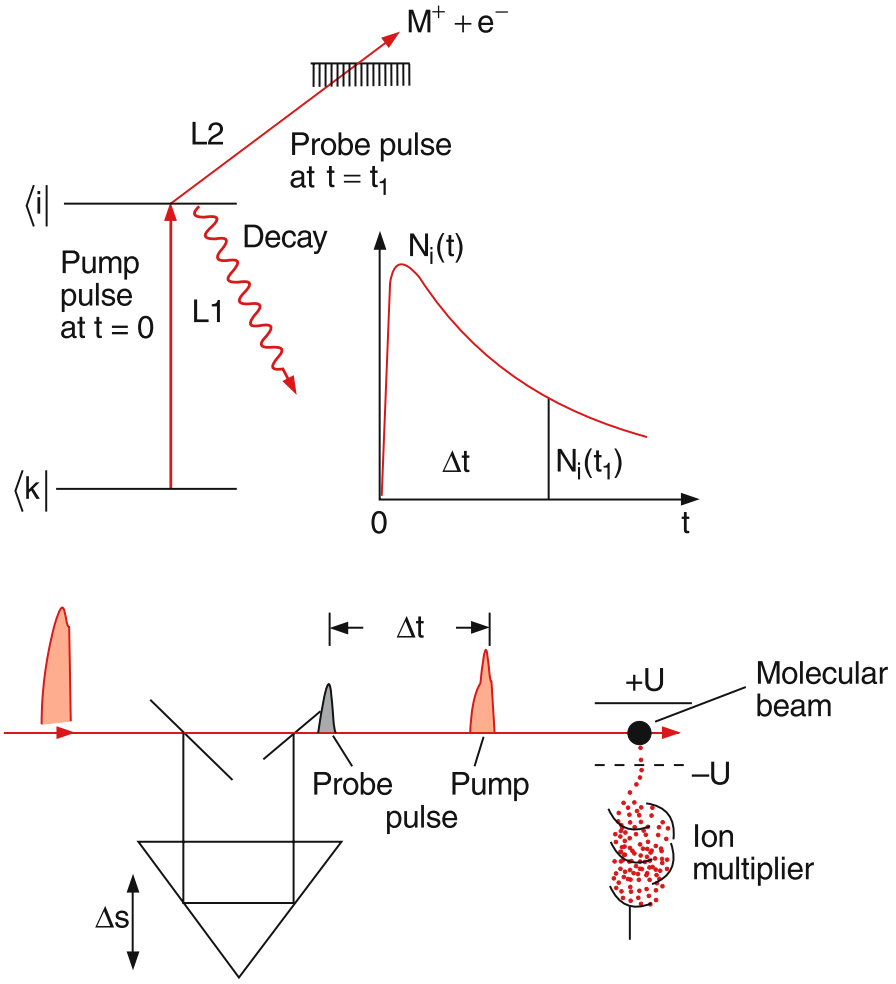

Pump-and-probe technique:

- Time resolution down to femtoseconds using femtosecond laser pulses
- Possible to synchronize due to the synchronous generation of the fluorescence by the pumping laser pulse.

Light emission, fluorescence

If an atom is excited (for instance by absorption of a photon, or by collisions with electrons) into a state with energy E_i above that of the ground state, it can spontaneously relax back into a lower state with energy E_j by emitting a photon $h\nu = E_i - E_j$. This spontaneous emission is called **fluorescence**. This lower state E_j may be still above the ground state E_k. In this case it can further relax into the ground state by photon emission or by a collision-induced transition.

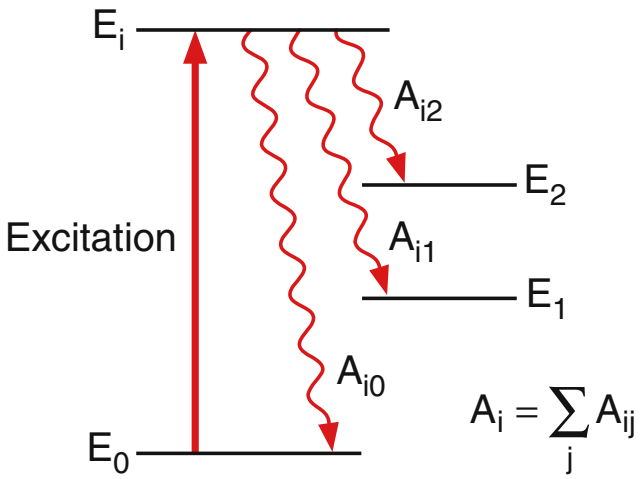

$$\mathrm{d}N_i = -A_{ij} N_i \, \mathrm{d}t$$

$$N_i(t) = N_i(0)\, \mathrm{e}^{-A_i t}$$

$$\tau_i = 1/A_i$$

$$\langle t_i \rangle = \frac{1}{N_0} \int_{N_0}^{0} t \cdot \mathrm{d}N_i(t)$$

$$= -\int_0^{\infty} t A_i \, \mathrm{e}^{-A_i t} \, \mathrm{d}t = \frac{1}{A_i} = \tau_i$$

After the mean lifetime $\langle t_i \rangle = \tau_i$ the initial population $N_i(t=0)$ has decreased to $N_i(0)/\mathrm{e}$.

Light emission, fluorescence

A classical oscillating electric dipole (Hertzian dipole) with electric dipole moment

$$\boldsymbol{p} = q\boldsymbol{r} = \boldsymbol{p}_0 \sin \omega t$$

emits the average power, integrated over all directions ϑ against the dipole axis (Fig. 7.3a) [5.2]

$$\overline{P} = \frac{2}{3} \frac{\overline{p^2}\omega^4}{4\pi\varepsilon_0 c^3} \quad \text{with} \quad \overline{p^2} = \frac{1}{2} p_0^2 \,. \tag{7.11}$$

In the quantum mechanical description, the average $\langle \boldsymbol{p} \rangle$ of the electric dipole moment of an atomic electron in state $(n, l, m_l, m_s) = i$ with stationary wave function ψ_i is given by the expectation value

$$\langle \boldsymbol{p} \rangle = e \langle \boldsymbol{r} \rangle = e \int \psi_i^* \boldsymbol{r} \psi_i \, \mathrm{d}\tau \,. \tag{7.12}$$

The vector $\boldsymbol{r}$ is the radius vector of the electron from the origin at the atomic nucleus (Fig. 7.3b).

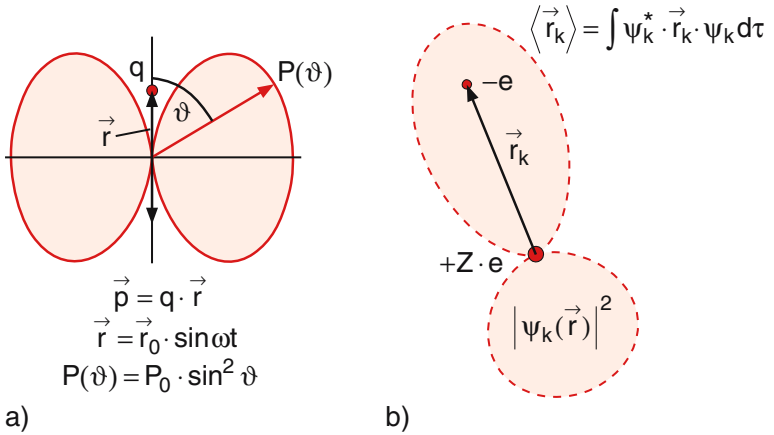

Fig. 7.3. (**a**) Spatial radiation characteristics of a classical oscillating electric dipole. (**b**) The expectation value $\langle p_k \rangle = -e\langle \boldsymbol{r}_k \rangle$ of the quantum mechanical dipole moment in level $|k\rangle$, determined by its wave function ψ_k

Light emission, fluorescence

For a transition $E_i \rightarrow E_k$ the wave functions of both states have to be taken into account, because the transition probability depends on both wave functions ψ_i and ψ_k. We therefore define the expectation value of the so-called ***transition dipole moment*** $M_{ik} = \langle p_{ik} \rangle$ as the integral

$$\boxed{\boldsymbol{M}_{ik} = e \int \psi_i^* \boldsymbol{r} \psi_k \, \mathrm{d}\tau} \quad , \tag{7.13}$$

where the two indices $i = (n_i, l_i, m_{l_i}, m_{s_i})$ and $k = (n_k, l_k, m_{l_k}, m_{s_k})$ are abbreviations for the four quantum numbers of each state.

Replacing the classical average $\overline{p^2}$ in (7.12) by the quantum mechanical expression

$$\frac{1}{2}\left(|M_{ik}| + |M_{ki}|\right)^2 = 2\,|M_{ik}|^2 \tag{7.14}$$

(see [7.1]), we obtain the average radiation power, emitted by an atom in level $\langle i|$ on the transition $\langle i| \rightarrow \langle k|$ as

$$\langle P_{ik} \rangle = \frac{4}{3} \frac{\omega_{ik}^4}{4\pi\varepsilon_0 c^3} |M_{ik}|^2 \, , \tag{7.15}$$

which is equivalent to the classical expression (7.11) for the radiation power of the Hertzian dipole, if the average $\overline{p^2}$ is replaced by $2|M_{ik}|^2$.

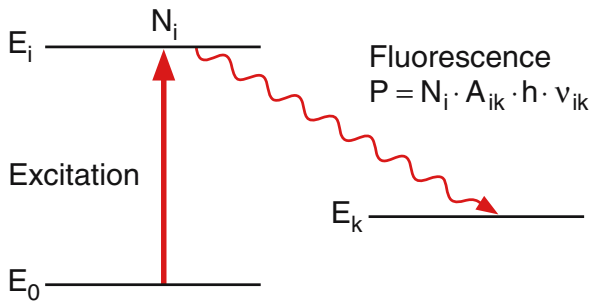

Fig. 7.4. Mean radiation power $\langle p_i k \rangle$ emitted by N_i excited atoms as fluorescence on the transition $|i\rangle \rightarrow |k\rangle$

N_i atoms in level $\langle i|$ emit the average radiation power $\langle P \rangle = N_i \langle P_{ik} \rangle$ on the transition $\langle i| \rightarrow \langle k|$ with frequency ω_{ik}.

Using the Einstein coefficient A_{ik} for spontaneous emission, which gives the probability per second that one atom emits a photon on the transition $\langle i| \rightarrow \langle k|$ the average power emitted by N_i atoms (Fig. 7.4) is

$$\langle P \rangle = N_i A_{ik} h \nu_{ik} = N_i A_{ik} \hbar \omega_{ik} \, . \tag{7.16}$$

The comparison of (7.15) with (7.16) yields the relation

$$A_{ik} = \frac{2}{3} \frac{\omega_{ik}^3}{\varepsilon_0 h c^3} |M_{ik}|^2 \tag{7.17a}$$

Radiative lifetime measurement

After the mean lifetime $\langle t_i \rangle = \tau_i$ the initial population $N_i(t=0)$ has decreased to $N_i(0)/\mathrm{e}$.

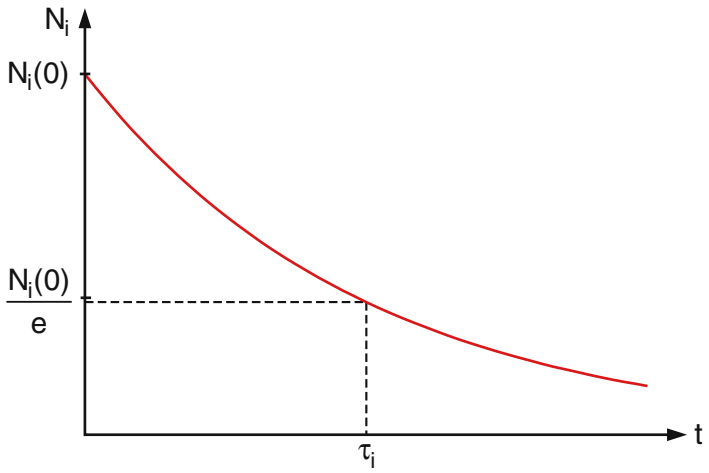

Fig. 7.14. Experimental decay curve of the population N_i of an excited level E_i with mean lifetime τ_i

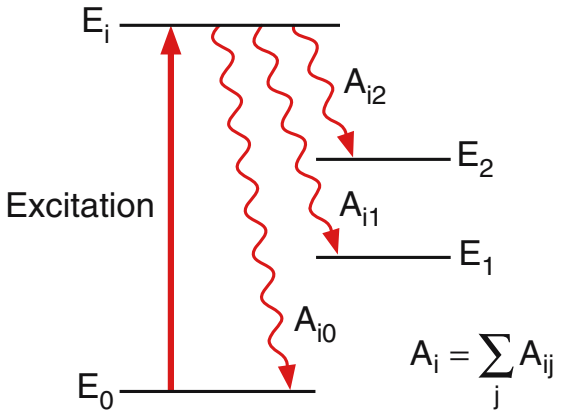

(j = n)

$$A_{in} = A_i \frac{I_{in}/(h\nu_{in})}{\sum_n I_{in}/(h\nu_{in})}$$

(k = n)

$$A_{ik} = \frac{2}{3}\frac{\omega_{ik}^3}{\varepsilon_0 h c^3}|M_{ik}|^2$$

Effective lifetime and quenching

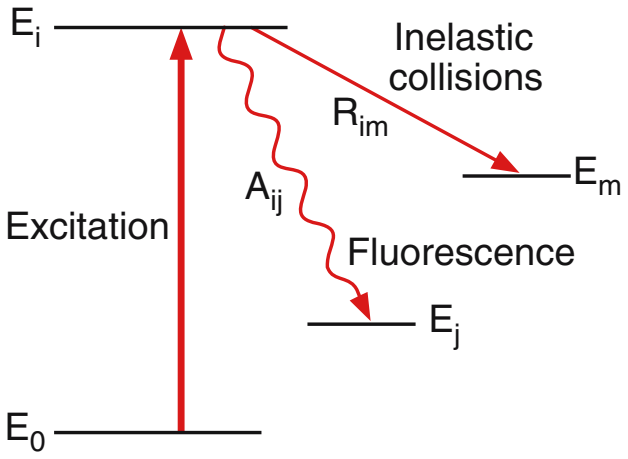

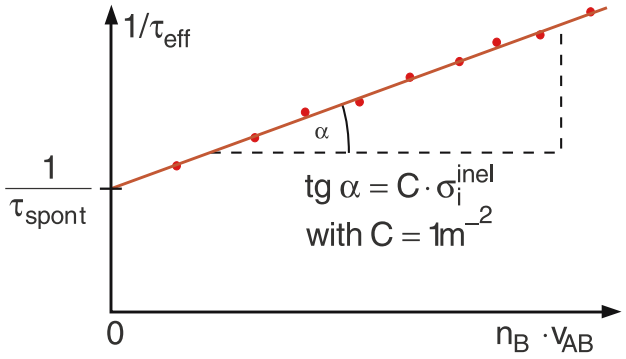

Fig. 7.16. Inverse effective lifetime $1/\tau_{\text{eff}}$ as a function of the density n_{B} of collision partners B (Stern–Volmer plot)

$$\mathrm{d}N_i = -(A_i + R_i)N_i \ \mathrm{d}t$$

$$\frac{1}{\tau_i^{\text{eff}}} = \frac{1}{\tau_i^{\text{spont}}} + \sigma_i^{\text{inel}} \sqrt{\frac{8}{\pi \mu k T}}\, p$$

Effective lifetime and quenching

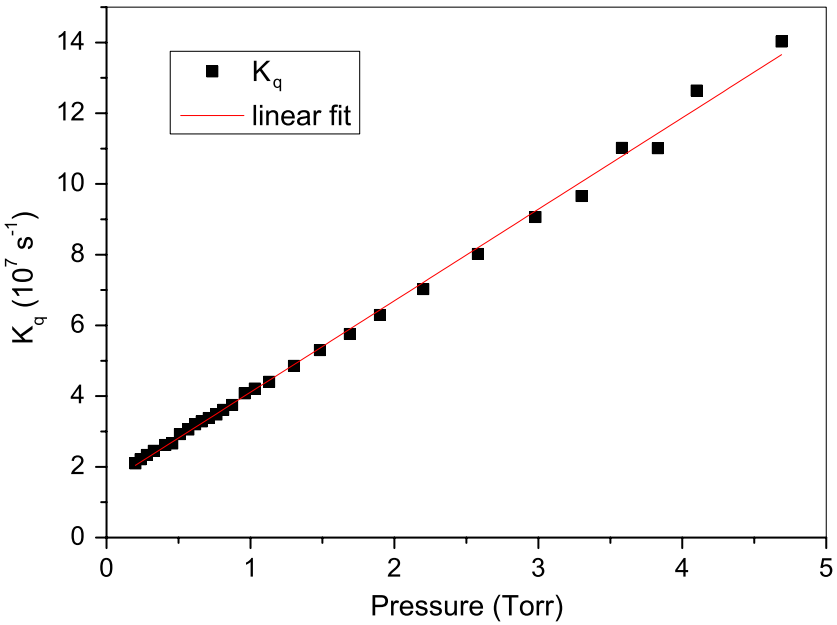

Figure 6. Stern–Volmer plot of the $N_2^+(B\,^2\Sigma_u^+, v = 0)$ quenching rate in pure N_2. The linear fit gives a slope of $(2.5871 \pm 0.027) \times 10^7$ Torr^{-1} s^{-1} and an intercept of $(1.5228 \pm 0.055) \times 10^7$ s^{-1}. The inverse of the intercept, $\tau = 65.67 \pm 2.37$ ns is in good agreement with the 62.33 ns radiative lifetime of [24].

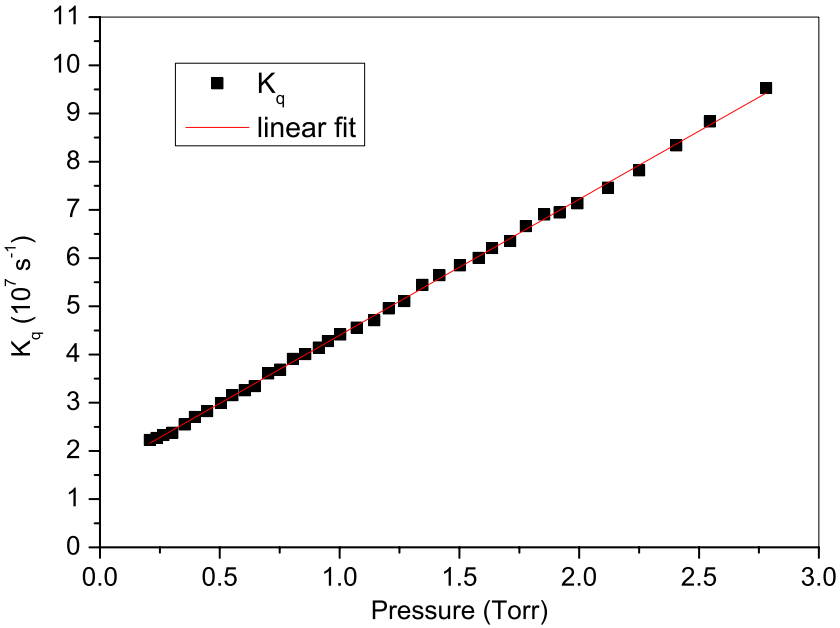

Figure 7. Stern–Volmer plot of the $N_2^+(B\,^2\Sigma_u^+, v = 0)$ quenching rate in N_2 + 50%O_2. The linear fit gives a slope of $(2.8236 \pm 0.0128) \times 10^7$ Torr^{-1} s^{-1} and an intercept of $(1.5752 \pm 0.0178) \times 10^7$ s^{-1}. The inverse of the intercept, $\tau = 63.48 \pm 0.72$ ns, is in good agreement with the 62.33 ns radiative lifetime of [24].

$$k_{\mathrm{mix}} = \frac{1}{2}k_{\mathrm{N_2}} + \frac{1}{2}k_{\mathrm{O_2}}$$

Dilecce et al. 2010 J.Phys.D

TC-SPC technique

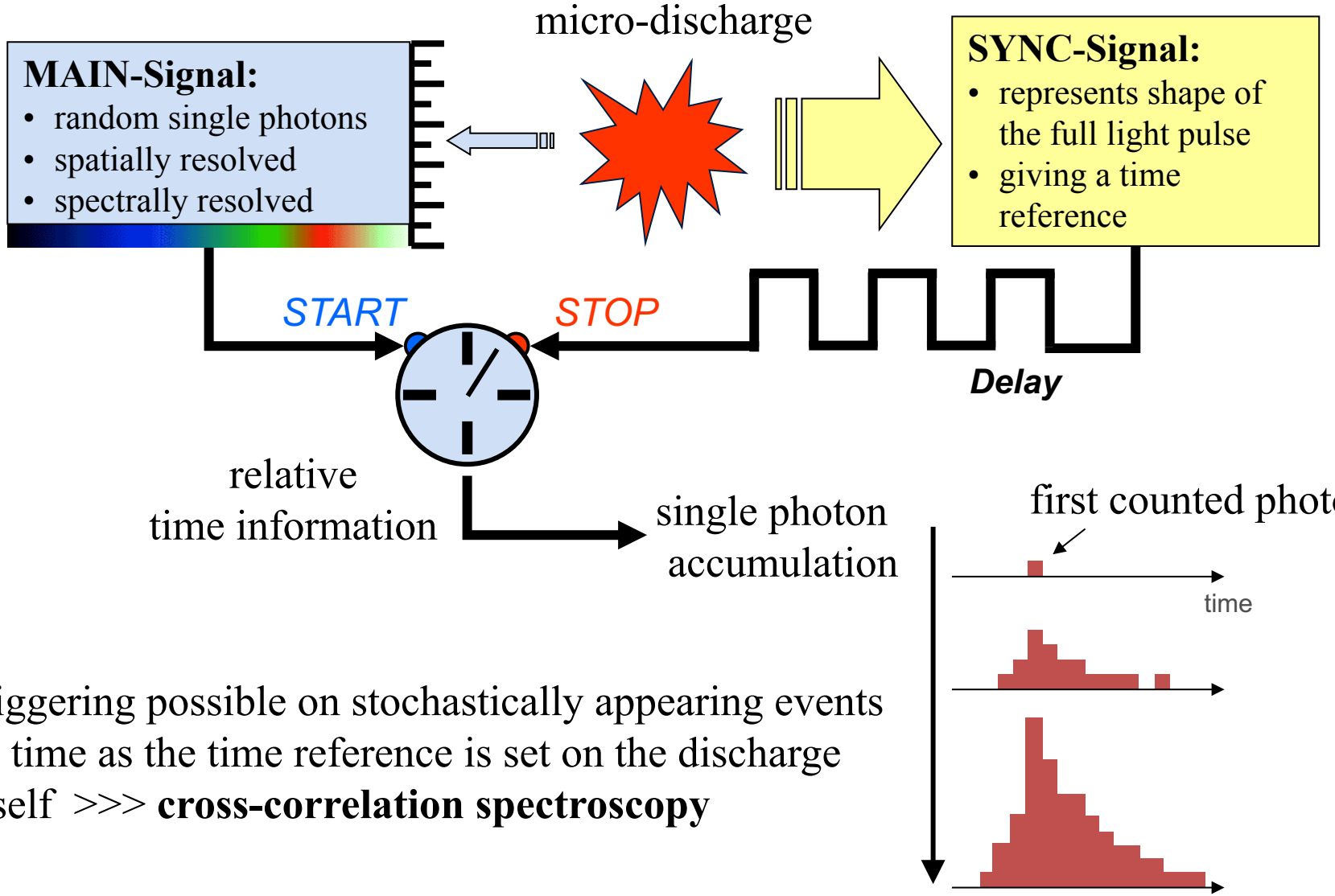

- triggering possible on stochastically appearing events in time as the time reference is set on the discharge itself >>> **cross-correlation spectroscopy**

Convolution >>> cross-correlation

1. Express each function in terms of a dummy variable τ.
2. Reflect one of the functions: $g(\tau) \rightarrow g(-\tau)$.
3. Add a time-offset, *t*, which allows $g(t-\tau)$ to slide along the τ-axis.
4. Start *t* at –∞ and slide it all the way to +∞. Wherever the two functions intersect, find the integral of their product. In other words, compute a sliding, weighted-sum of function $f(\tau)$, where the weighting function is $g(-\tau)$.

The resulting waveform (not shown here) is the convolution of functions *f* and *g*.

If *f*(*t*) is a unit impulse, the result of this process is simply *g*(*t*), which is therefore called the impulse response. Formally:

$$\int_{-\infty}^{\infty} \delta(\tau)\, g(t-\tau)\, d\tau = g(t)$$

wiki

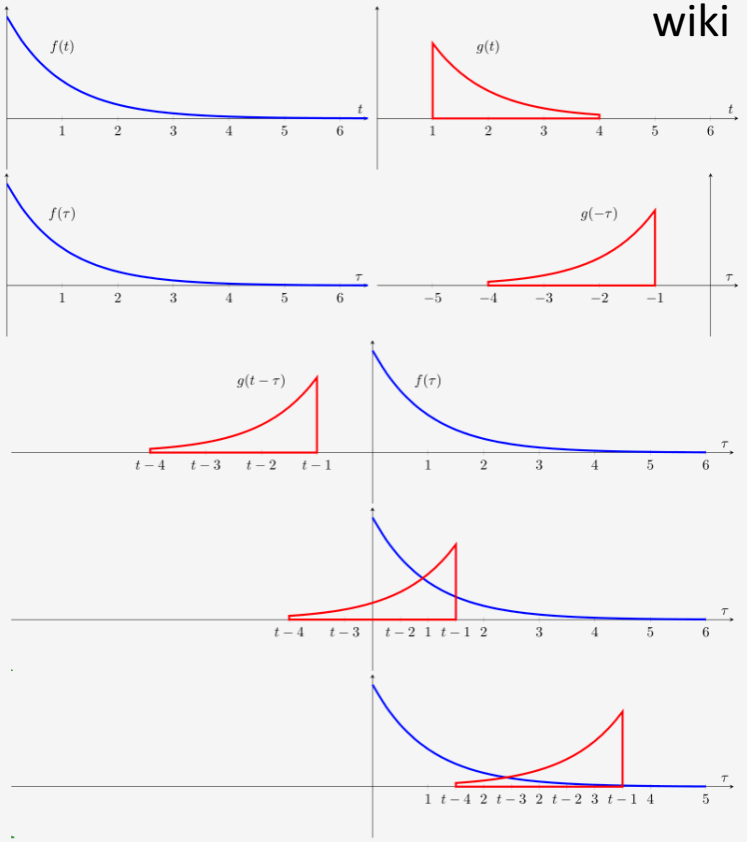

$$(f \star g)(t) \stackrel{\text{def}}{=} \overline{f}(-t) * g(t)$$

$$(f \star g)(\tau) \stackrel{\text{def}}{=} \int_{-\infty}^{\infty} \overline{f}(t) g(\tau + t) \mathrm{d}t$$

$$(f \star g)(\tau) \stackrel{\text{def}}{=} \sum_{t=-\infty}^{\infty} f(t) g(\tau + t)$$

(δ-fce)

TC-SPC statistics basics 1

$$w_i = qz_i$$

Photoelectrons generated by impinged photons on the cathode with given quantum efficiency.

$$p_l(i) = \frac{(w_i)^l}{l!} e^{-w_i} \qquad \sum_{l=0}^{\infty} p_l = 1$$

The probability of emission of *l* photoelectrons in the *i*-th interval is given by the **Poisson distribution**.

$$p_0(i) = e^{-w_i}$$

$$p_1(i) = w_i e^{-w_i}$$

$$p_{l>1}(i) = 1 - p_0(i) - p_1(i)$$

$$= 1 - e^{-w_i} - w_i e^{-w_i}$$

$$= 1 - (1 + w_i) e^{-w_i}.$$

The Taylor series of the exponential function is $(1-w_i+w_i^2/2+\ldots)$, we take the first two.

TCSPC statistics scheme

N_A number of counts in i-th interval

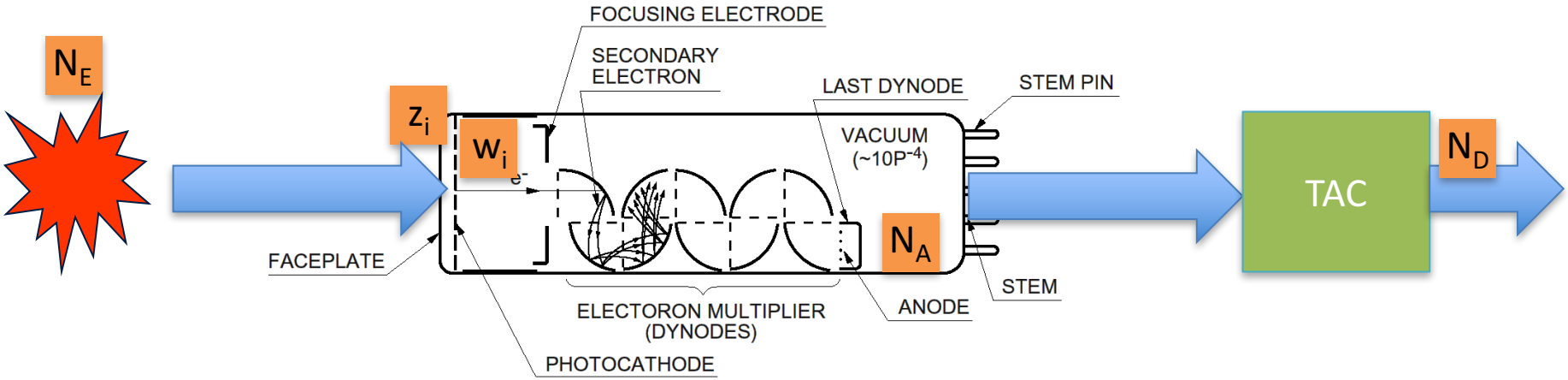

if $N_D \ll N_E$ it follows that $N_i = N_A$

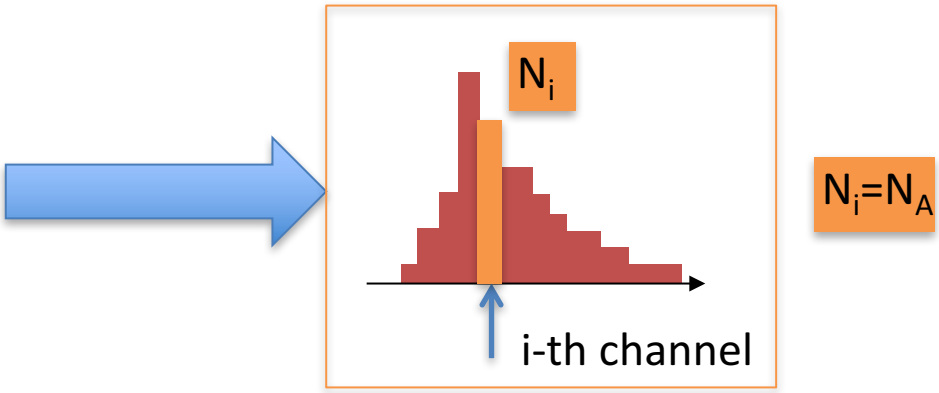

TC-SPC statistics basics 2

$$N_A = N_E[p_1(i) + p_{i>1}(i)]$$

If $w_i \ll 1$, then $p_1(i) = w_i$

After a large number of excitation pulses N_E, the number of anode pulses N_A in the i-th interval.

After developing to Taylor series, as shown before:

$$p_{i>1}(i) = w_i^2 \ll w_i$$

And it follows:

$$\begin{aligned} N_A &\approx N_E(w_i + w_i^2) \\ &\approx N_E w_i \\ &= N_E q z_i. \end{aligned}$$

Therefore the number of anode pulses N_A is proportional to the intensity of the fluorescence at time t_i.

TCSPC statistics scheme

N_A number of counts in i-th interval

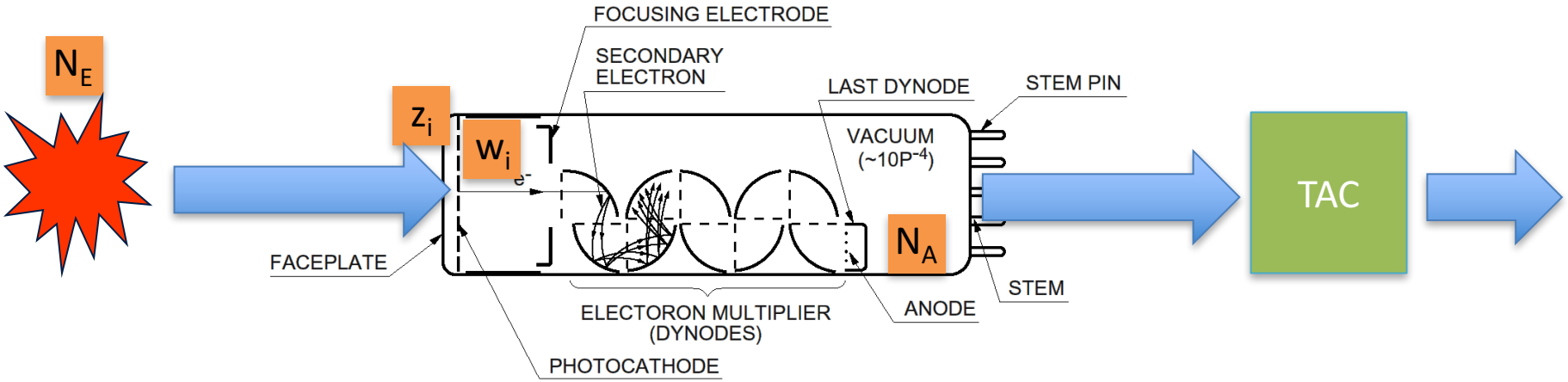

if $N_D \ll N_E$ it follows that $N_i = N_A$

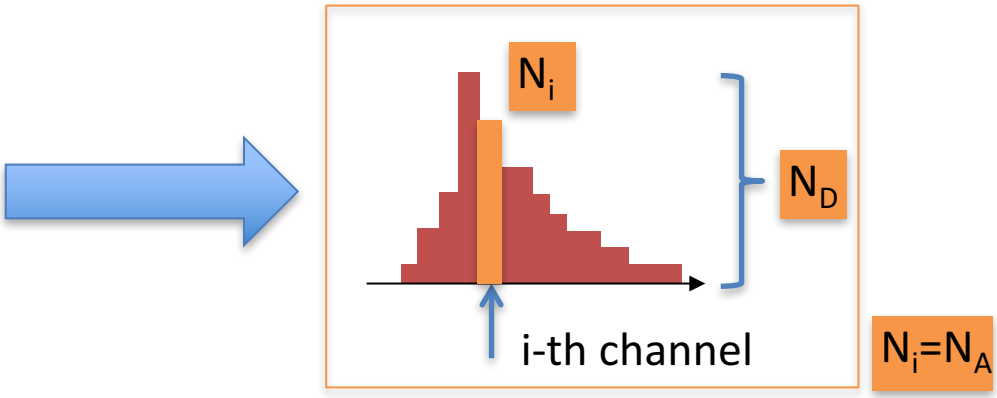

TC-SPC statistics basics 3

$$N_A \approx N_E(w_i + w_i^2)$$
$$\approx N_E w_i$$
$$= N_E q z_i.$$

Relation of N_A to number of Counts in the i-th channel N_i:

$$N_A = \frac{N_i}{1 - \frac{1}{N_E}\sum_{j=1}^{i-1} N_j}$$

Because the TAC detects only the first photon in given time interval for a given excitation cycle, **N_A is not the number of counts in the i-th channel N_i.** The true relation is given left.

number of *detected* anode pulses

$$\sum_j N_j \leqslant N_D$$

if $N_D \ll N_E$ it follows that $N_i = N_A$

Consequently the count in channel i is a measure of the fluorescence intensity at time t_i.

TC-SPC statistics basics 4

Generally, N_D is measured at the output of the TAC and N_D/N_E kept below a certain limit. If N_D is not very much less than N_E, data can be corrected using Equation 2.10 provided that $w_i \ll 1$ (see Section 6.4). Collection at high N_D/N_E ratios need not lead to distorted curves if pile-up inspection is performed (see Section 5.2.5(b)). However, it is simpler and probably just as efficient, when data transfer and analysis are taken into account, to keep the ratio N_D/N_E below a certain value.

PILE-UP effect

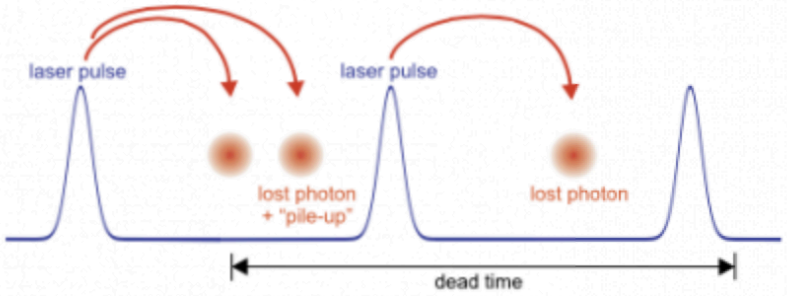

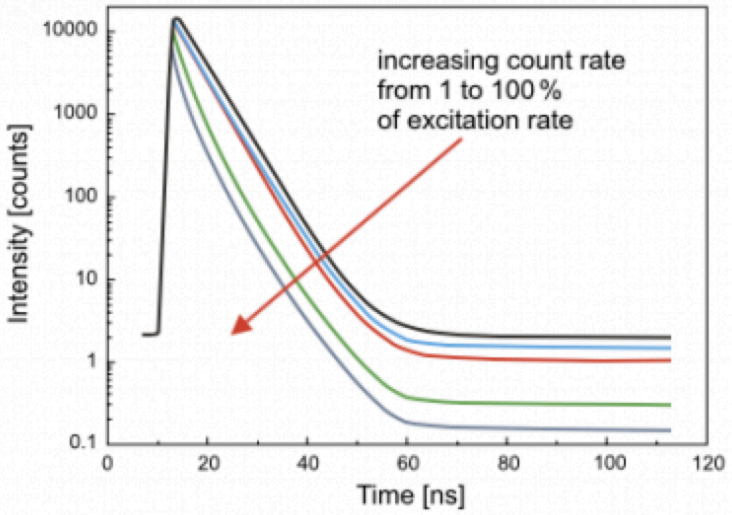

Other issues to be aware of

- Color effect (consequence of photoeffect)
- Afterpulsing (consequence of PMT setup)
- Ultra-short reflections
- …

Sensitivity and precision

- The effect of **PMT noise** is greatly reduced by the mode of TAC operation
  >>> enhanced Signal-to-Noise ratio (up to 100x noise reduction)

- **Noise due to the dark counts on PMT** (cooling, background subtraction …)

- **Noise due to the counting error**, number of counts in each channel $I(t_i)$ follows a Poisson distribution with a standard deviation σ_i given by $\sigma_i=(I(t_i))^{1/2}$
- It follows that **to have 5% precision** in the number of N_i counts in *i*-th channel, where the the curve decayed to 1% of its maximum value, one has: $0.05=1/\sigma_i=1/(N_i)^{1/2}$ and N_i is 400, that means one has to measure 40000 counts in maximum
- **Signal-to-Noise ratio** is given as well by the Poisson distribution and is equal to the standard deviation:

$$SNR = \sqrt{N_i}$$

- Dynamic range (ratio between the largest and smallest value of measured quantity): for **ICCD typically** 1000:1, **streak** 10000:1, for **TCSPC** usually 100000:1 and more

Comparison

Fundamental comparison of TCSPC, Gated II-CCD and Streak

	TCSPC	Gated II-CCD	Streak
Recording method	Records temporal traces, but only at a single wavelength at spectra, but only at a single wave-length at a time. The spectral axis must be scanned sequentially.	Records full spectra, but only at a single time position at a time. The time axis must be sampled sequentially.	Records full 2-dimensional time-resolved spectra simultane-ously, without any scanning.
Can exploit high rep-rate sources	yes	no	yes
Can exploit low rep-rate sources	no	yes	yes
Yields Poisson statistics	yes	no	yes
Typical lifetime ranges	ps to ns	ns to ms	sub-ps to ms

Hamamatsu News 2009

PMT and MCP structure

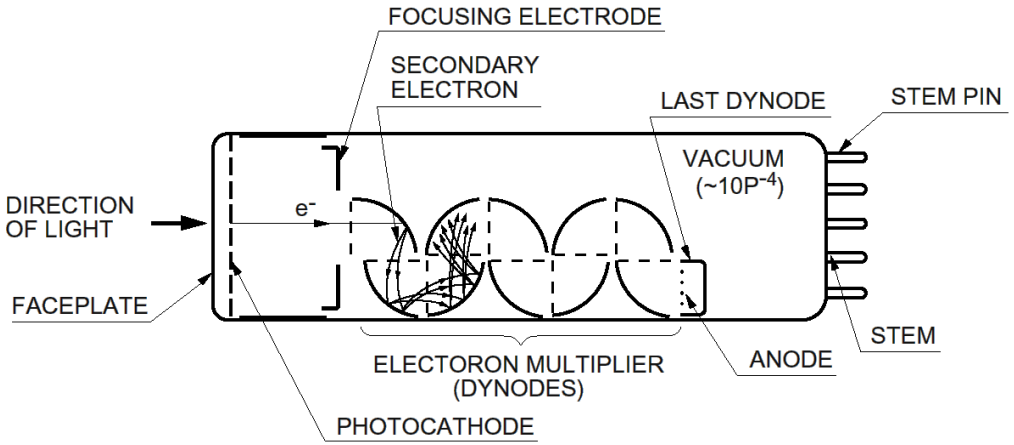

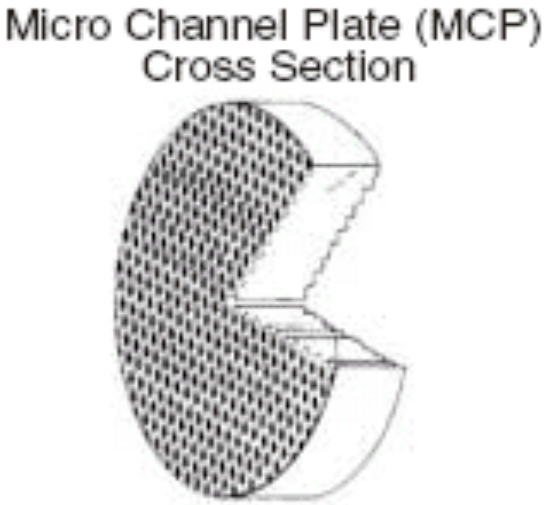

Gain of up to 10^8

PMT resolution, transit time

Leading edge discrimination

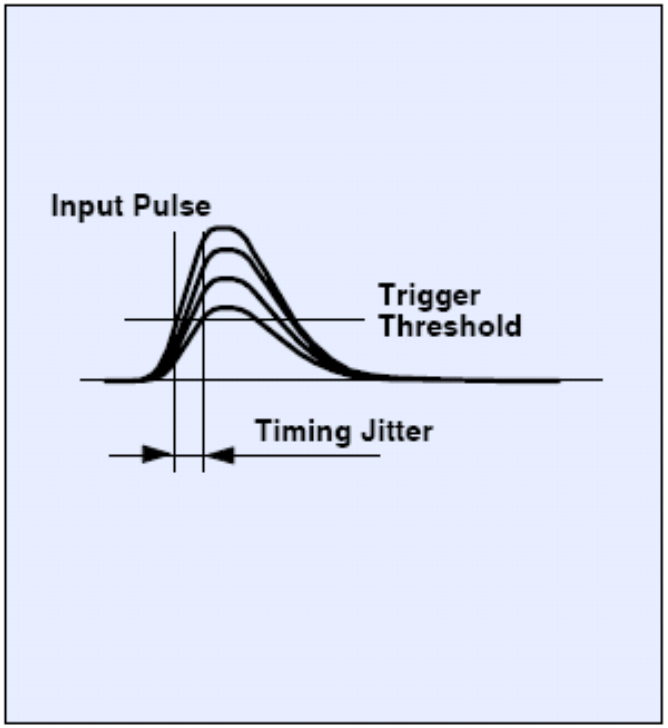

CFD

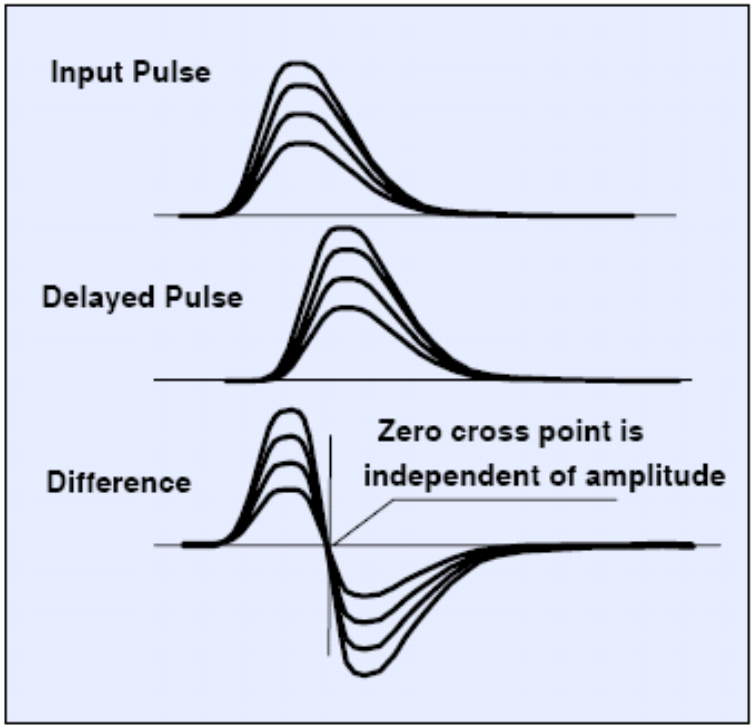

pulse-height-induced timing jitter avoided

Becker 2006 Advanced TCSPC techniques

PMT resolution, transit time

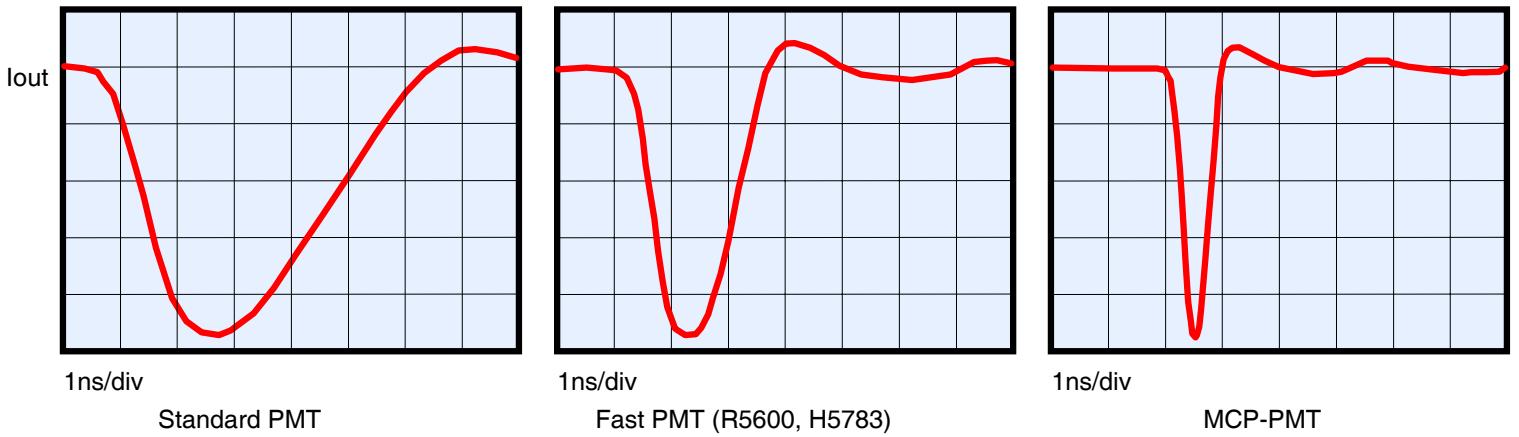

Fig. 175: Single electron response (SER) of different photomultipliers

Due to the random nature of the detector gain, the pulse amplitude varies from pulse to pulse.

Becker 2006 Advanced TCSPC techniques

PMT transit time spread

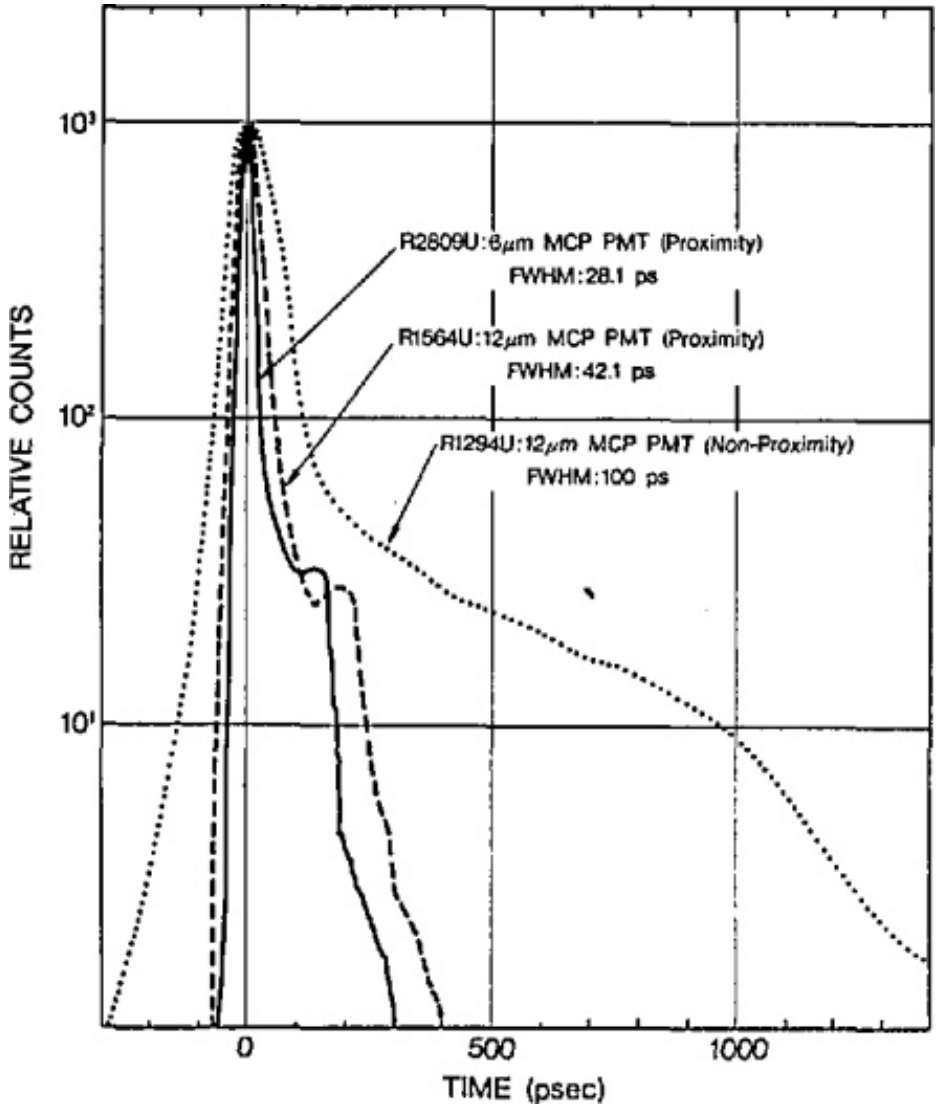

PMT transit

Table 4.1. Transient Time Spreads of Conventional and MCP PMTs[a]

Photomultiplier		Configuration (upper freqeuncy)	TTS (ns)	Dynode
Hamamatsu	R928	Side-on (300 MHz)[b]	0.9	9 stage
	R1450	Side-on	0.76	10 stage
	R1394	Head-on	0.65	10 stage
	R7400	Compact PMT, TO-8 (900 MHz)	300 ps	–
	H5023	Head-on (1 GHz)	0.16	10 stage
RCA	C31000M	Head-on	0.49	12 stage
	8852	Head-on	0.70	12 stage
Philips	XP2020Q	Head-on	0.30	12 stage
Hamamatsu	R1294U	Nonproximity MCP-PMT	0.14	2 MCP
	R1564U	Proximity focused MCP-PMT, 6 micron (1.6–2 GHz)	0.06	2 MCP
	R2809U	Proximity MCP-PMT, 6 micron	0.03[d]	2 MCP
	R3809U	Proximity MCP-PMT Compact size, 6 micron	0.025[d]	2 MCP
	R2566	Proximity MCP-PMT with a grid, 6 micron (5 GHz)[c]	–	2 MCP

[a]Revised from [81].
[b]Numbers in parentheses are the approximate frequencies where the response is 10% of the low-frequency response. The H5023 has already been used to 1 GHz.
[c]From [86].
[d]From [87].

Lakowicz 2006 Principles of fluorescence spectroscopy

TC-SPC review

light intensity > 0.01 to 0.1 photons per signal period → Pile-Up Problem

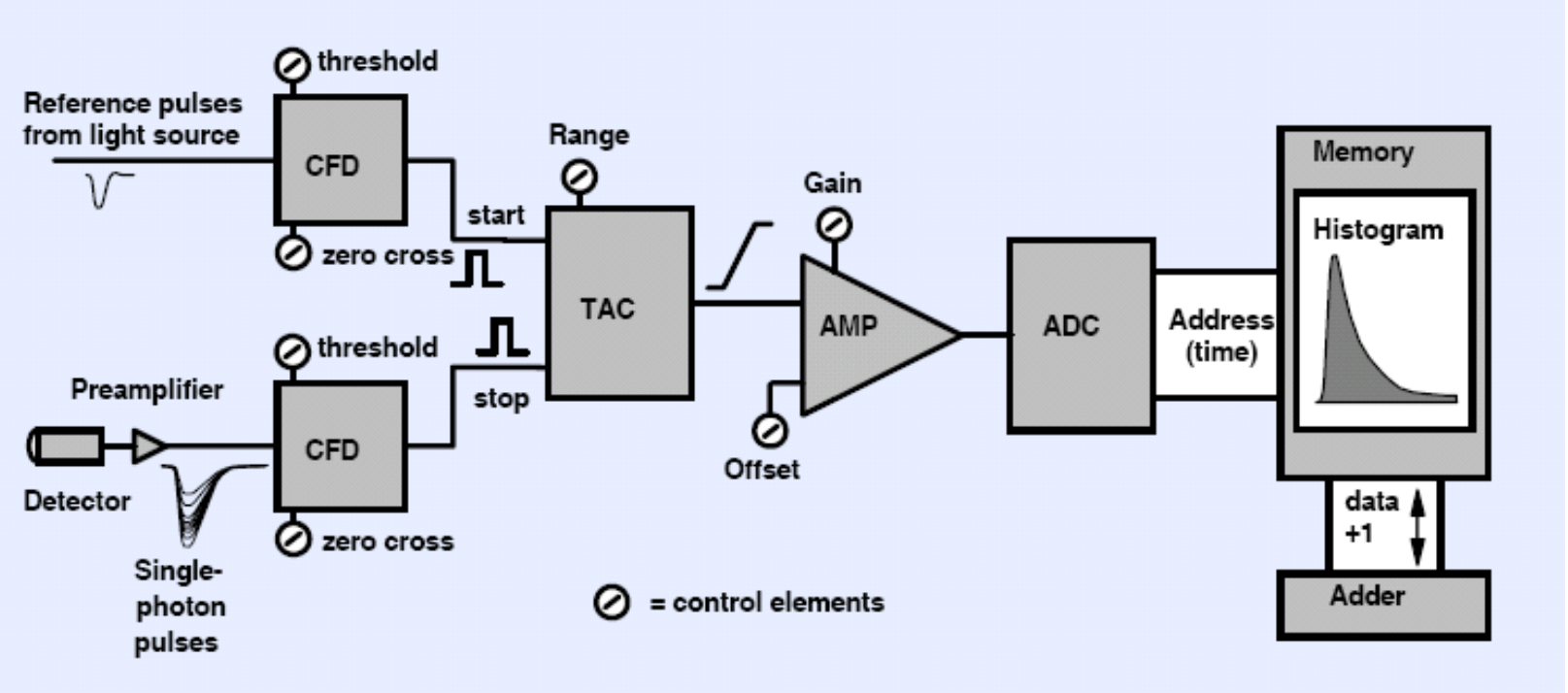

Relatively slow recording speed and long data acquisition times

→ high repetition rates and low dead time (approx. 100 ns; i.e. 10^7 photons/s)

Becker 2006 Advanced TCSPC techniques

Use in plasma-physics and signal synchronization

- **Short discharges with high repetition**:

  rf discharges, barrier discharges, Trichel pulsing corona, mw discharges, self-pulsing sparks
- **Synchronization** via light pulse, current pulse, laser excitation or TTL of applied voltage waveform

Kinetic scheme dependent example

- Streamer discharges generated in atmospheric pressure air
- Spectra is dominated by the second positive system of molecular nitrogen
- Relatively weak bands of first negative system are present as well

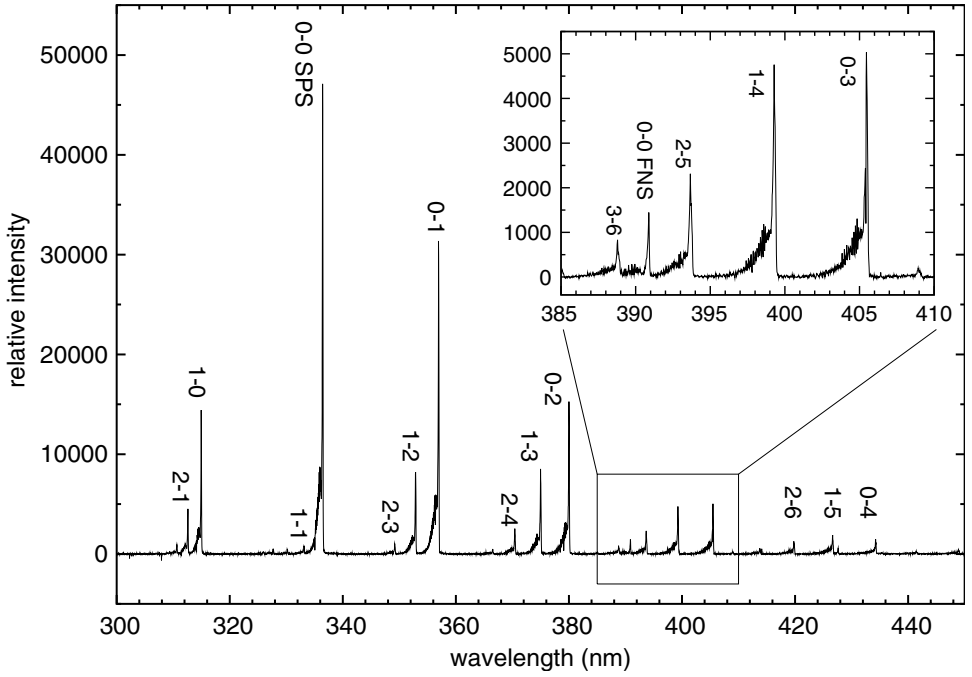

Kinetic scheme dependent example

- Streamer discharges generated in atmospheric pressure air
- Spectra is dominated by the second positive system of molecular nitrogen
- Relatively weak bands of first negative system are present as well

$$\mathrm{e} + \mathrm{N_2}(\mathrm{X}^1\Sigma_g^+)_{\upsilon=0} \longrightarrow \mathrm{N_2^+}(\mathrm{B}^2\Sigma_u^+)_{\upsilon'=0} + 2\mathrm{e}, \qquad \triangle\mathrm{E} = 18.7\ \mathrm{eV};$$

$$\mathrm{e} + \mathrm{N_2}(\mathrm{X}^1\Sigma_g^+)_{\upsilon=0} \longrightarrow \mathrm{N_2}(\mathrm{C}^3\Pi_u)_{\upsilon'=0} + \mathrm{e}, \qquad \triangle\mathrm{E} = 11.0\ \mathrm{eV};$$

$$\mathrm{N_2^+}(\mathrm{B}^2\Sigma_u^+)_{\upsilon'=0} \rightarrow \mathrm{N_2^+}(\mathrm{X}^2\Sigma_u^+)_{\upsilon''=0} + \mathrm{h}\nu,\ \lambda = 391.5\ \mathrm{nm}, \tau_0^{\mathrm{B}} = 64.0\ \mathrm{ns}$$

$$\mathrm{N_2}(\mathrm{C}^3\Pi_u)_{\upsilon'=0} \rightarrow \mathrm{N_2}(\mathrm{B}^3\Pi_g)_{\upsilon''=0} + \mathrm{h}\nu,\ \lambda = 337.1\ \mathrm{nm}, \tau_0^{\mathrm{C}} = 36.6\ \mathrm{ns}$$

$$\mathrm{N_2^+}(\mathrm{B}^2\Sigma_u^+)_{\upsilon'=0} + \mathrm{N_2/O_2} \rightarrow \mathrm{products},\ \tau_{\mathrm{eff}}^{\mathrm{B}} = 0.045\ \mathrm{ns}$$

$$\mathrm{N_2}(\mathrm{C}^3\Pi_u)_{\upsilon'=0} + \mathrm{N_2/O_2} \rightarrow \mathrm{products},\ \tau_{\mathrm{eff}}^{\mathrm{C}} = 0.640\ \mathrm{ns}$$

Kinetic scheme dependent example

- Streamer discharges generated in atmospheric pressure air

$$\frac{\mathrm{d}n_{\mathrm{B}}(x,t)}{\mathrm{d}t} = k_{\mathrm{B}}(E/N)n_{\mathrm{N_2}}n_{\mathrm{e}}(x,t) - \frac{n_{\mathrm{B}}(x,t)}{\tau_{\mathrm{eff}}^{\mathrm{B}}}$$

$$\frac{\mathrm{d}n_{\mathrm{C}}(x,t)}{\mathrm{d}t} = k_{\mathrm{C}}(E/N)n_{\mathrm{N_2}}n_{\mathrm{e}}(x,t) - \frac{n_{\mathrm{C}}(x,t)}{\tau_{\mathrm{eff}}^{\mathrm{C}}}$$

$$\frac{\dfrac{\mathrm{d}I_{\mathrm{B}}(r,t)}{\mathrm{d}t} + \dfrac{I_{\mathrm{B}}(r,t)}{\tau_{\mathrm{eff}}^{\mathrm{B}}}}{\dfrac{\mathrm{d}I_{\mathrm{C}}(r,t)}{\mathrm{d}t} + \dfrac{I_{\mathrm{C}}(r,t)}{\tau_{\mathrm{eff}}^{\mathrm{C}}}} \frac{\tau_{\mathrm{eff}}^{\mathrm{B}}}{\tau_{\mathrm{eff}}^{\mathrm{C}}} = R_{\mathrm{FNS/SPS}}(E/N)$$

Trichel pulse corona

- Breakdown in negative corona Trichel pulse

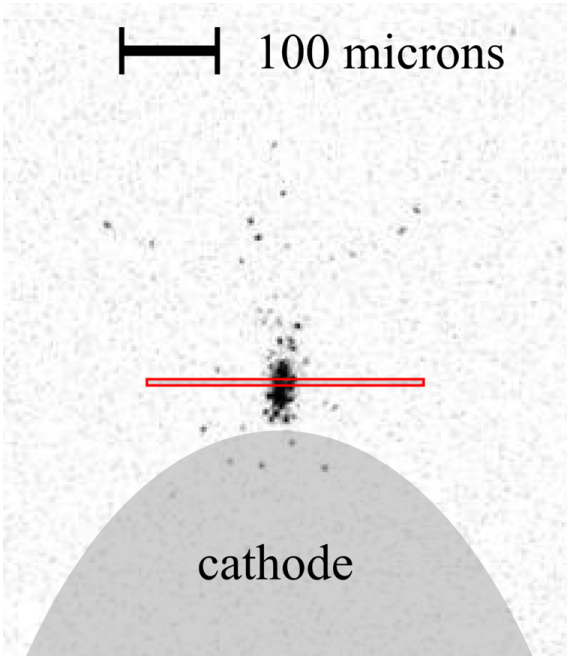

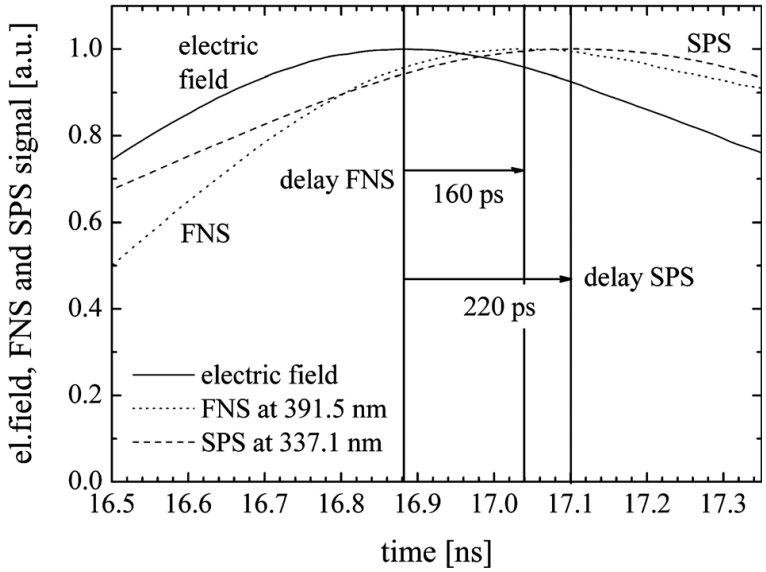

FIG. 3. Experimentally obtained FNS and SPS signals of positive streamer in its early stage together with determined electric field development for Trichel pulse in negative corona discharge.[41] Delays of the FNS and SPS signals maxima to the electric field maximum are denoted. The uncertainty of the obtained delay values is not worse than ±20 ps.

Setup for corona and calibration

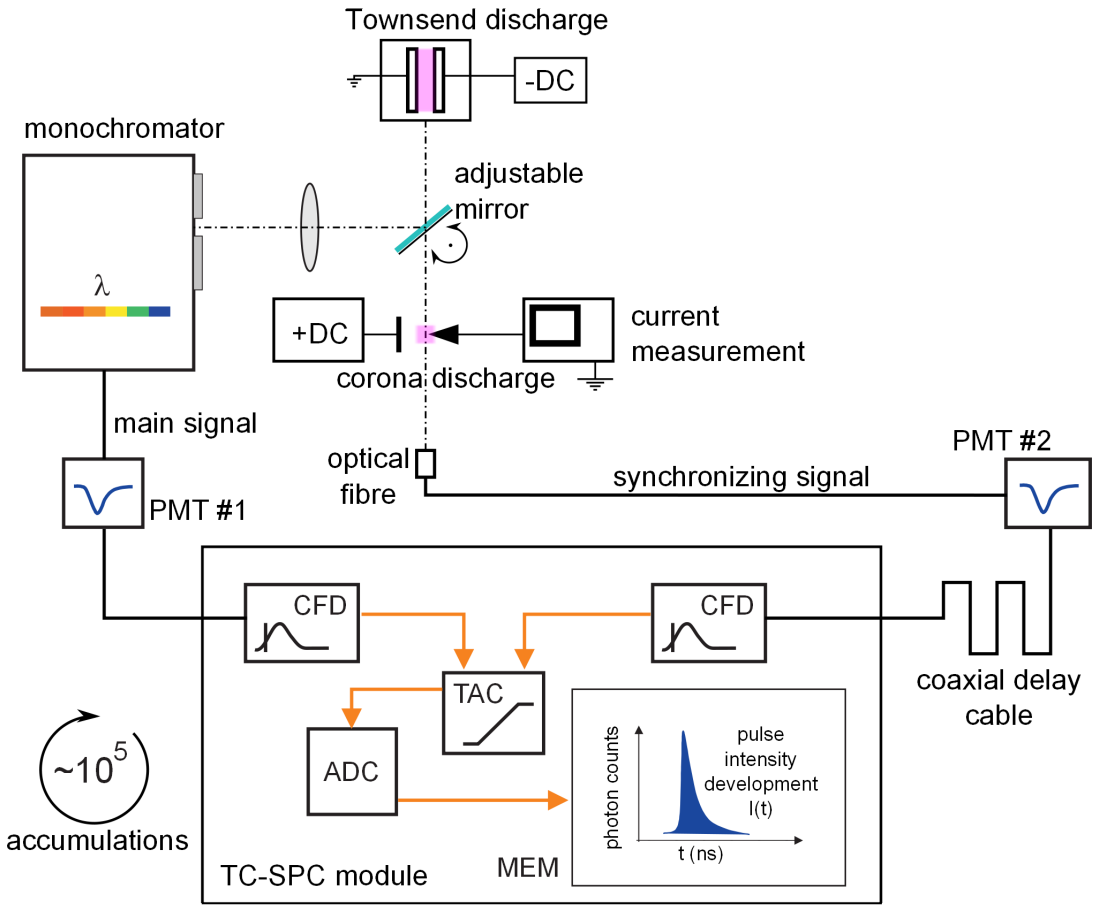

Figure 1: Experimental setup for the E/N determination in TP discharge. DC: direct current power supply; PMT: photomultiplier; CFD: constant fraction discriminator; TAC: time-to-amplitude converter; ADC: analog-to-digital converter.

Calibration

- Streamer discharges generated in atmospheric pressure air

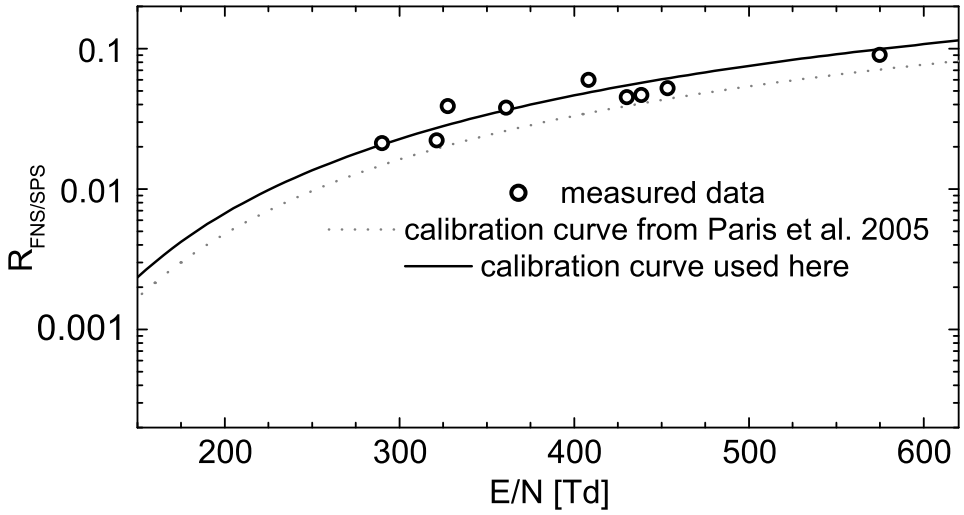

Trichel pulse electric field

SPS

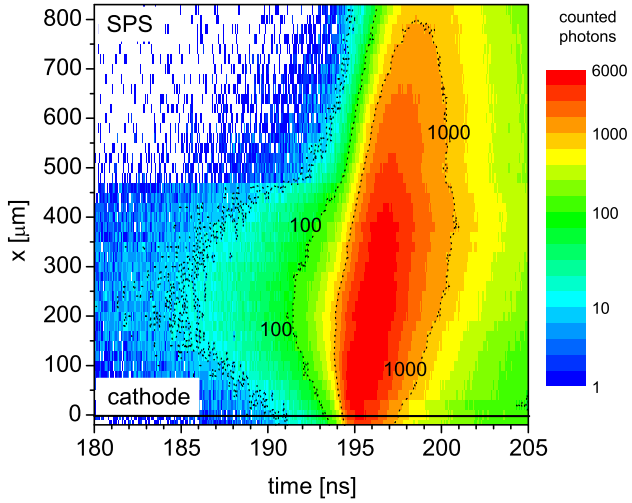

FNS

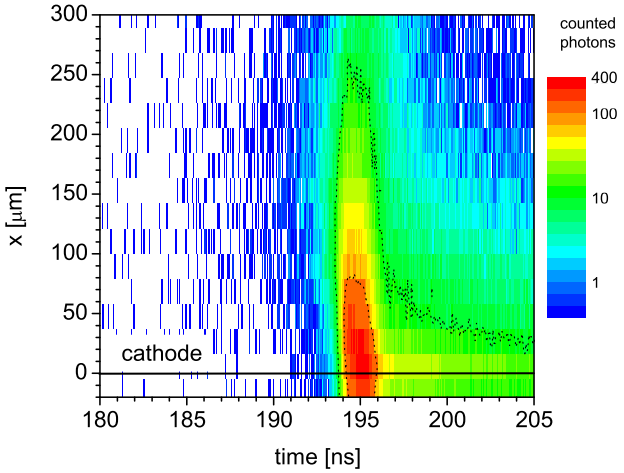

$$1\,\mathrm{Td} = 10^{-21}\,\mathrm{Vm}^2$$

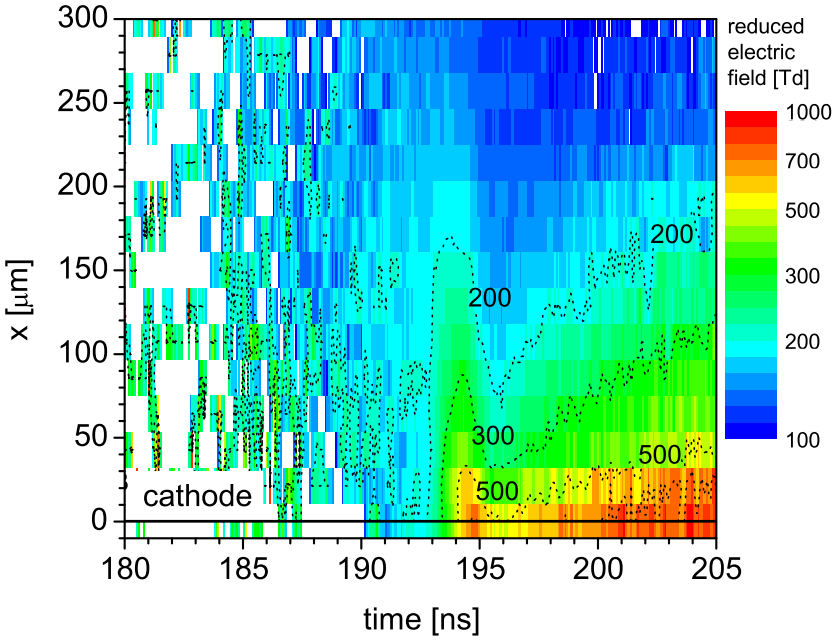

Limits for TCSPC on streamers

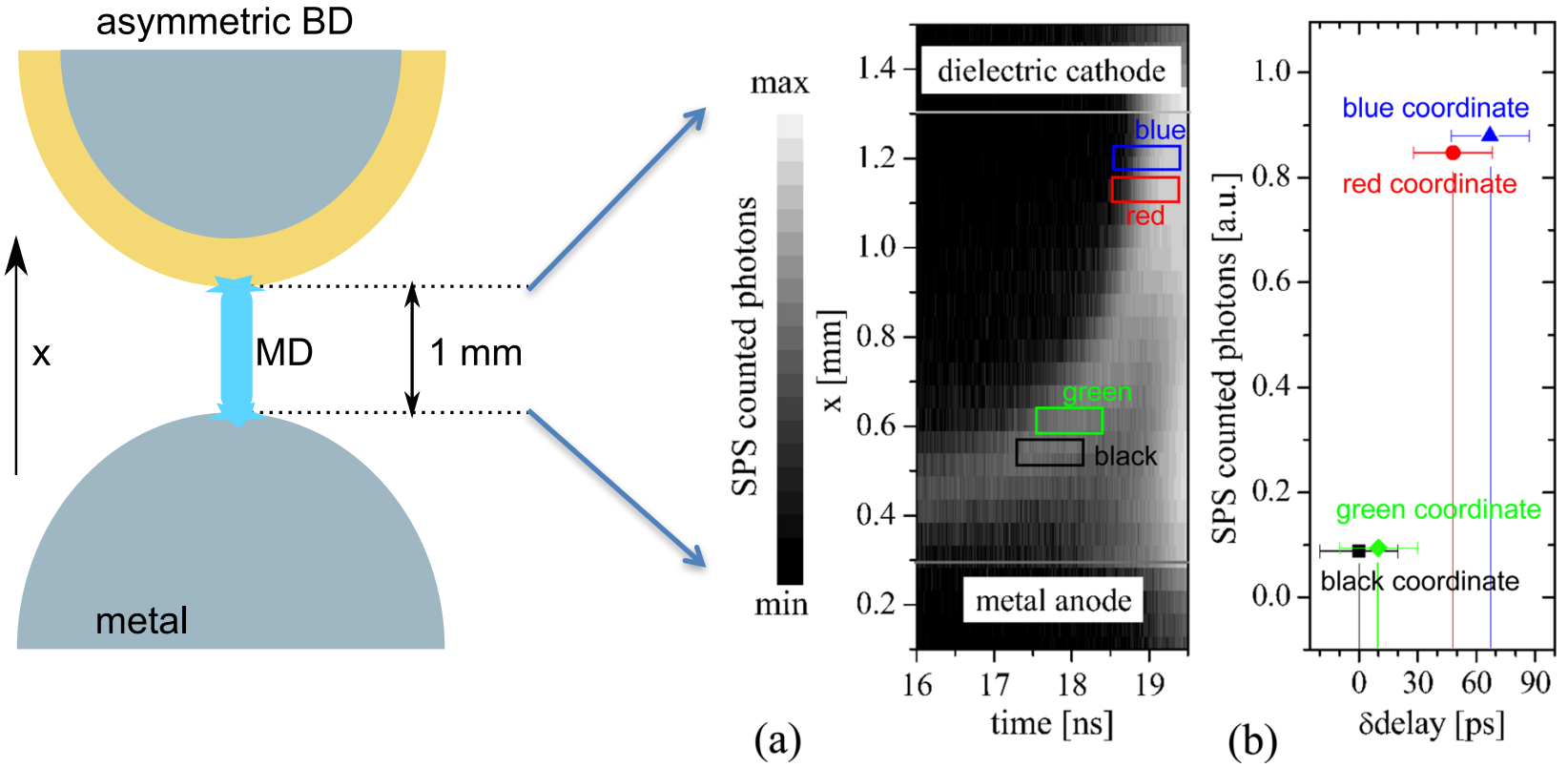

FIG. 4. Experimentally obtained SPS signal of positive streamer propagating towards dielectric cathode in barrier discharge arrangement[42] with depicted coordinates for the estimation of the delay dilatation (a). The dilatation of the delay *δdelay* as well as the increase of the emitted intensity of the SPS signal from the streamer head is shown in part (b).

Quantum mechanics based example

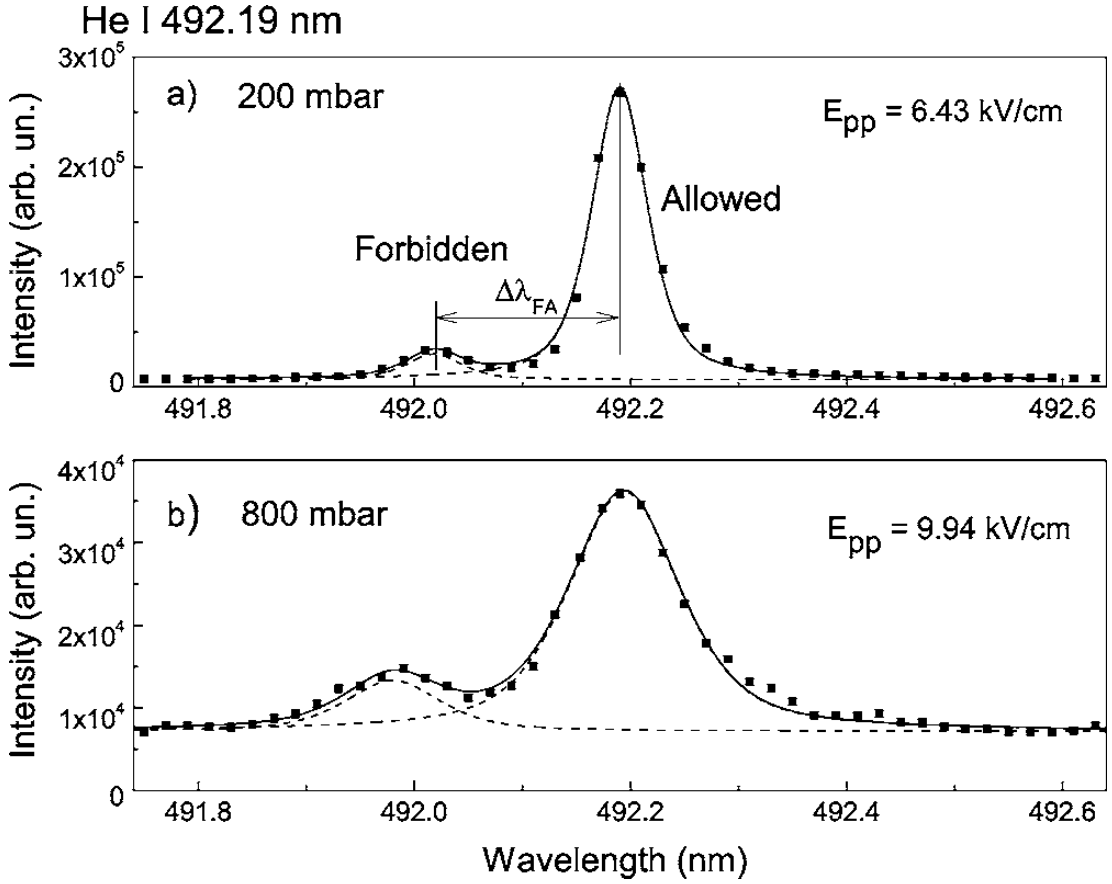

FIG. 2. Typical π polarized spectra of the He I 492.1 nm line and its forbidden counterpart. Discharge conditions: (a) 200 mbar and U_{gap}=490 V; (b) 800 mbar and U_{gap}=670 V.

Obradovic 2008 APL

Quantum mechanics based example

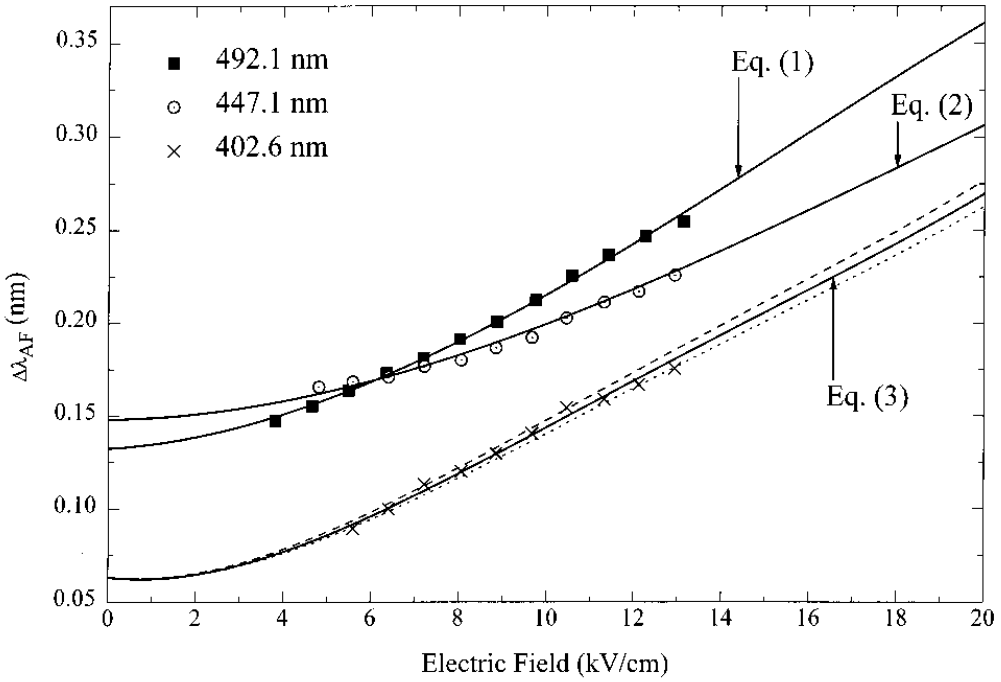

FIG. 2. The polynomial best fits of the calculated wavelength separation $\Delta\lambda_{AF}$ of π components of the 402.6 nm line and its forbidden line: $m_{upper}=0\rightarrow m_{lower}=0$ transition (dashed line), $m_{upper}=1\rightarrow m_{lower}=1$ transition (dotted line) and average between $m=0$ and $m=1$ displacements, Eq. (3) (solid line). For the 492.1 nm and 447.1 lines only average values [solid lines, Eqs. (1) and (2), respectively] are given. The results (scattered graphs) of the experimental testing of Eqs. (1)–(3), obtained by measuring $\Delta\lambda_{AF}$ for all three He I lines vs electric field strength determined from the π shape of H_β profile in helium–hydrogen mixture, are also given.

Kuraica 1997 APL

RF discharge in helium at 1atm

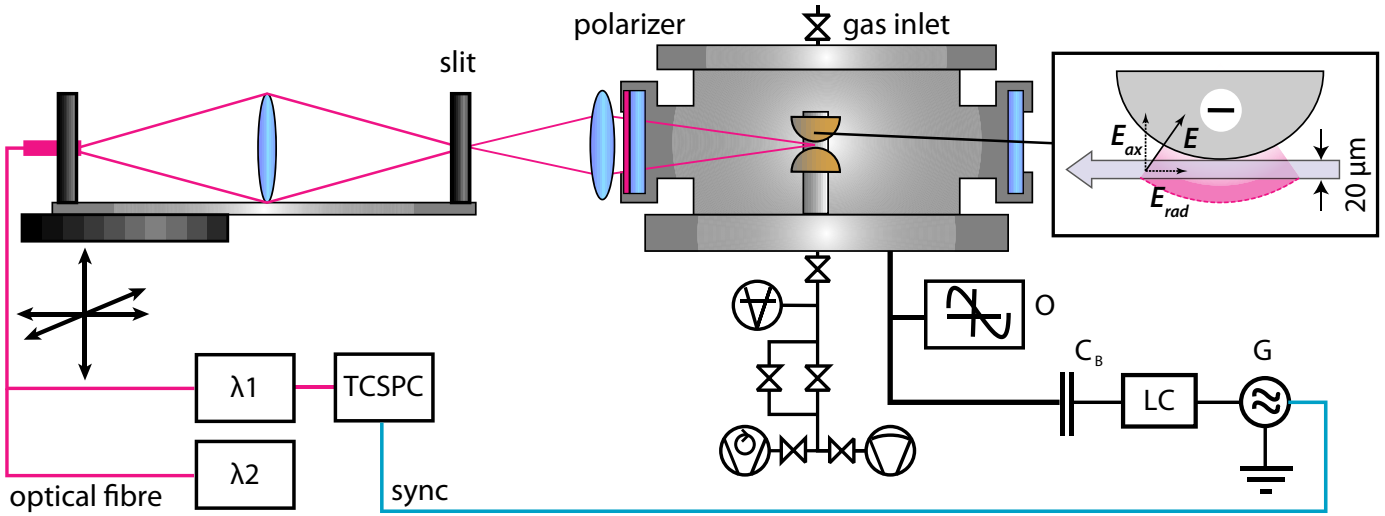

Quantum mechanics based example

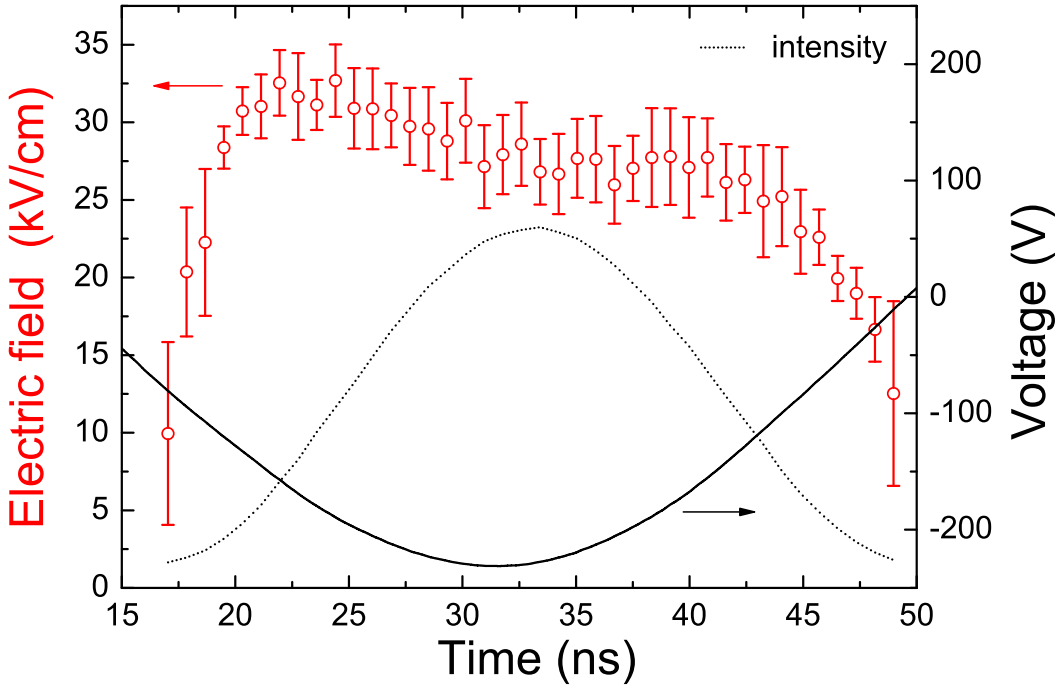

Figure 5. Time-development of electric field strength at the driven electrode obtained from the fit of forbidden and field-free component. Solid and the dotted line denote the applied RF voltage development and the development of intensity integrated over the spectral profile, respectively.

Navratil 2015 TCSPC results

Summary

- The principles and technical realization of the TCSPC technique were introduced
- The measured fluorescence from the atomic/molecular transitions was followed back to its origin
- Selected examples of quantitative high-resolution spectroscopy were presented